A DIRECT METHOD FOR THE MEASUREMENT OF CONTROL ROD WORTH IN A NUCLEAR REACTOR

Thesis for the Degree of M. S. MICHIGAN STATE UNIVERSITY WILLIAM ARTHUR EMSLIE 1972







90(4)

.

-

ABSTRACT

A DIRECT METHOD FOR THE MEASUREMENT OF CONTROL ROD WORTH IN A NUCLEAR REACTOR

By

William Arthur Emslie

It is often necessary to perform control rod calibration in a nuclear reactor. Such calibration requires the measurement of the reactivity produced when discrete sections of a control rod are withdrawn from a critical reactor pile. From these data a total reactivity worth curve can be complied for the length of the rod. The subject of this thesis is the development of a means by which reactivity worth can be measured.

A solution to this measurement problem has been developed using the current output of a compensated ionization chamber (adjacent to the reactor) as a signal source. When a section of control rod is withdrawn from a critical reactor, the current from the ion chamber is

$$i_s(t) = I_0 e^{t/\theta}$$

where t is time, θ_p is the reactor stable period and \mathbf{I}_0 is the initial ion chamber current.

The stable period is proportional to the amount of reactivity produced since

$$\theta_{\rm p} = \frac{\theta_{\rm 0}}{k_{\rm ex}} \cong \frac{\theta_{\rm 0}}{\rho}$$

 θ_0 is the mean neutron lifetime, k_{ex} is the excess multiplication factor and ρ is the reactivity. This approximate relationship between θ_p and ρ makes it possible to obtain the reactivity from the output current of the ion chamber since

$$i_s(t) = I_0 e^{t/\theta} \cong I_0 e^{\rho t/\theta}$$

Actual measurement of $\,\rho\,$ is accomplished with a circuit composed of a logarithmic amplifier followed by a differentiator and filter. The transfer function of this circuit is

$$V_{\text{out}}(s) = V_1(s) \frac{(-R_1C_2s)}{(R_1C_1s+1)(R_2C_2s+1)} \frac{1}{(R_fC_fs+1)}$$

where $V_1(s)$ is the frequency domain expression for $V_1(t)$ (the output voltage of the logarithmic amplifier) and is equal to

$$V_1(s) = \frac{-A \log_{10}(I_0/I_k)}{s} - \frac{A \log_{10}e}{\theta_p s^2}$$

In the time domain, the logarithm of the ion chamber current produces a linear ramp voltage $v_1(t)$ where

$$v_1(t) = -A \log_{10} \frac{i_s(t)}{I_k} = -A \log_{10} \frac{I_0 e^{t/\theta_p}}{I_k} = -A \log_{10} \frac{I_0}{I_k} - \frac{At}{\theta_p} \log_{10} e^{t/\theta_p}$$

This ramp voltage is then differentiated and filtered to obtain a d-c voltage proportional to the inverse of ρ . The resulting voltage (V_2) is

$$v_2 = -K \frac{d}{dt} (v_1(t)) = -K \frac{d}{dt} (-A \log_{10} \frac{I_0}{I_k} - \frac{At}{\theta_p} \log_{10} e)$$

= $\frac{KA}{\theta_p} \log_{10} e \cong \frac{\rho KA}{\theta_0} \log_{10} e$

V₂ may be calibrated on a d-c voltmeter to indicate the corresponding reactivity.

A circuit to synthesize the transfer function was designed and constructed. Results of tests made on circuit performance show the total accuracy in the measurement of $\,\rho\,$ to be within $\pm\,0.5\,$ percent of the meter scale.

A DIRECT METHOD FOR THE MEASUREMENT OF CONTROL ROD WORTH IN A NUCLEAR REACTOR

Ву

William Arthur Emslie

A THESIS

Submitted to
Michigan State University
in partial fulfillment of the requirements
for the degree of

MASTER OF SCIENCE

Department of Electrical Engineering and Systems Science

TO MY PARENTS

ACKNOWLEDGMENTS

The author wishes to express his sincere thanks to his major professor, Dr. G.L. Park, for his guidance and support during the course of the research. Sincere appreciation is also expressed to the other members of the guidance committee, Dr. B. Wilkinson for his advice on nuclear reactor theory and Dr. L. Giacoletto for his guidance on the design of the reactivity measuring circuit.

Special thanks is extended to Mr. E. Brockbank who made possible extensive testing and calibration of the reactivity meter.

TABLE OF CONTENTS

		Page
	LIST OF TABLES	v
	LIST OF FIGURES	vi
	LIST OF SYMBOLS	viii
Chapter		
I.	INTRODUCTION	1
II.	REACTOR TRANSIENT BEHAVIOR	5
	2.1 Reactivity, Reactor Period and Theoretical Relationships	5
	2.2 Relationship Between Reactivity and the Reactor Stable Period	7
	2.3 Effects of Prompt and Delayed Neutrons on	
	Reactor Transient Behavior	7 11
	2.4 The Compensated Ion Chamber	11
III.	DESIGN OF THE REACTIVITY MEASURING DEVICE	15
	3.1 Formulation of the Problem	15
	3.2 Possible Methods of Solution	16
	3.3 The Circuit and Theory of Operation	20
	3.4 Calibration	23
IV.	CONSTRUCTION OF THE REACTIVITY METER	27
	4.1 Circuit Tests, Performance and	
	Specifications	27
v.	CONCLUSIONS	30
BIBLIOGRAP	ну	32
APPENDIX A	DESIGN OF THE LOGARITHMIC AMPLIFIER	33
APPENDIX B	DETERMINATION OF THE RAMP FREQUENCY COMPONENTS	39
APPENDIX C	DESIGN OF THE DIFFERENTIATOR	42
APPENDIX D	DESIGN OF THE FILTER	47
APPFNDTY F	CDECTETCATIONS OF THE COMPENSATED TON CHAMBED	/ ₁ Q

LIST OF TABLES

Table		Page
4.1	Specifications of the reactivity meter	29
A.1	Electrical specifications of the Burr-Brown modular logarithmic amplifier model 4116 (current input only)	34
E.1	Specifications of the Westinghouse type WL-8501 compensated ion chamber	49

LIST OF FIGURES

Figure		Pa ge
1.1	Calibration curve for the shim rod in the Michigan State University TRIGA Mark I muclear reactor	3
2.1	Relationship between reactivity and reactor stable period for the Michigan State University TRIGA Mark I nuclear reactor (Courtesy of Gulf General Atomic)	8
2.2	Combined effect of prompt and delayed neutrons in a supercritical reactor	10
2.3	Simplified diagram of a compensated ion chamber .	12
2.4	Graph of ion chamber output current as a function of reactor output power level for the Michigan State University TRIGA Mark I nuclear reactor	14
3.1	Block diagram of a circuit which provides a d-c voltage proportional to the inverse of the reactor stable period	16
3.2	Circuit for obtaining a d-c voltage proportional to θ_p	17
3.3	Circuit for obtaining a discrete voltage proportional to the slope of $i_s(t)$	18
3.4	Circuit diagram of the reactivity measuring instrument	21
3.5	Apparatus used to calibrate the reactivity meter	24
3.6	Graph showing the relationship between reactivity and reactor stable period for the Michigan State University TRIGA Mark I nuclear reactor (Courtesy of Gulf General Atomic)	26
4.1	Photographs of the reactivity meter	28
A.1	Burr-Brown modular logarithmic amplifier model	35

Figure		Page
A.2	Design curves for the Burr-Brown model 4116 log amplifier, (a) Reference current vs. R, (b) Voltage constant vs. R,	37
C.1	Transfer function plot for an ideal differentiator, (a) Imaginary part, (b) Real part	42
C.2	Transfer function plot for a compensated differentiator, (a) Imaginary part, (b) Real part	43
c.3	Equivalent circuit of a compensated differentiator	44
D.1	Output filter for the reactivity meter	47

LIST OF SYMBOLS

A	Voltage constant for log amplifier
Α ₀ (ω)	Open loop voltage gain
С	Capacitance
¹ 0	Initial ion chamber output current
I _k	Reference current for log amplifier
Is	Ion chamber output current
^k eff	Reactor effective multiplication factor
k ex	Reactor excess multiplication factor
n	Neutron
P	Reactor power level
P ₀	Initial reactor power level
R	Resistance
t	Time
v	Voltage
Z	Impedance
β	Beta particle
$\boldsymbol{\beta_i}$	Fraction of delayed fission neutrons in the ith group
Υ	Gamma photon
θ_{0}	Mean neutron lifetime
$\theta_{\mathbf{d}}$	Reactor power level doubling time
$\theta_{\mathbf{p}}$	Reactor stable period
θ _t	Minimum ramp "on" time

- λ_i Decay constant of ith group
 - ρ Excess reactivity (reactivity)
 - A Reactor neutron flux
- Φ_0 Initial reactor neutron flux
- ω Radian frequency

CHAPTER I

INTRODUCTION

The necessity to perform calibration of the control rods in a nuclear reactor requires a means by which to measure the reactivity produced by withdrawal of discrete sections of a control rod from a critical reactor pile.

Use of an ionization chamber adjacent to the reactor provides an exponential current $(i_s(t))$ from which the reactivity may be derived. When a section of control rod is withdrawn from a critical reactor $i_s(t)$ becomes

$$i_s(t) = I_0 e^{t/\theta} p$$
 (1.1)

where \mathbf{I}_0 is the initial ion chamber current, t is time and θ_p is the reactor stable period. 1

The reactivity may be obtained from equation (1.1) since

$$\theta_{\mathbf{p}} \cong \frac{\theta_{\mathbf{0}}}{\rho} \tag{1.2}$$

where θ_0 is the mean neutron lifetime.²

The reactor stable period used in this expression is the time required for the ion chamber current $(i_s(t))$ to increase by a factor of e.

This approximation is explained and justified in Section 2.1.

The relationship between ρ and $i_g(t)$ expressed in Equations (1.1) and (1.2) makes it possible to obtain ρ from $i_g(t)$. This may be accomplished by means of a circuit which first takes the logarithm of $i_g(t)$ and then differentiates and filters the result to yield a d-c voltage proportional to ρ .

An example of a control rod calibration curve is illustrated in Figure 1.1. The curve is compiled by withdrawing the rod a short distance and measuring the corresponding reactivity produced. This procedure is repeated until the entire length of the rod has been withdrawn.

Chapter II of this study details the theory underlying reactivity and the ionization chamber. The effects of prompt and delayed neutrons are also discussed.

In Chapter III the reactivity measurement problem is formulated with a set of possible solutions. A particular solution method from these alternatives is then presented. Analysis of the design, mathematical properties, and calibration of the circuit follows. Further design analysis is presented in the Appendices.

$$1 \text{ dollar} = \frac{k_{\text{ex}}}{\beta_{i}} \cong \frac{\rho}{\beta_{i}}$$
 (1.3)

where k_{ex} is the reactor excess multiplication factor and β_i is a normalizing constant equal to the total fraction of delayed neutrons and varies with different reactors. For the Michigan State University TRIGA Mark 1 reactor β_i = 0.0073 and therefore one dollar's worth of reactivity is that amount required to produce an excess multiplication factor of 0.0073.

The units of reactivity as expressed in Figure 1.1 are in dollars and cents where 1 dollar = 100 cents and is defined as

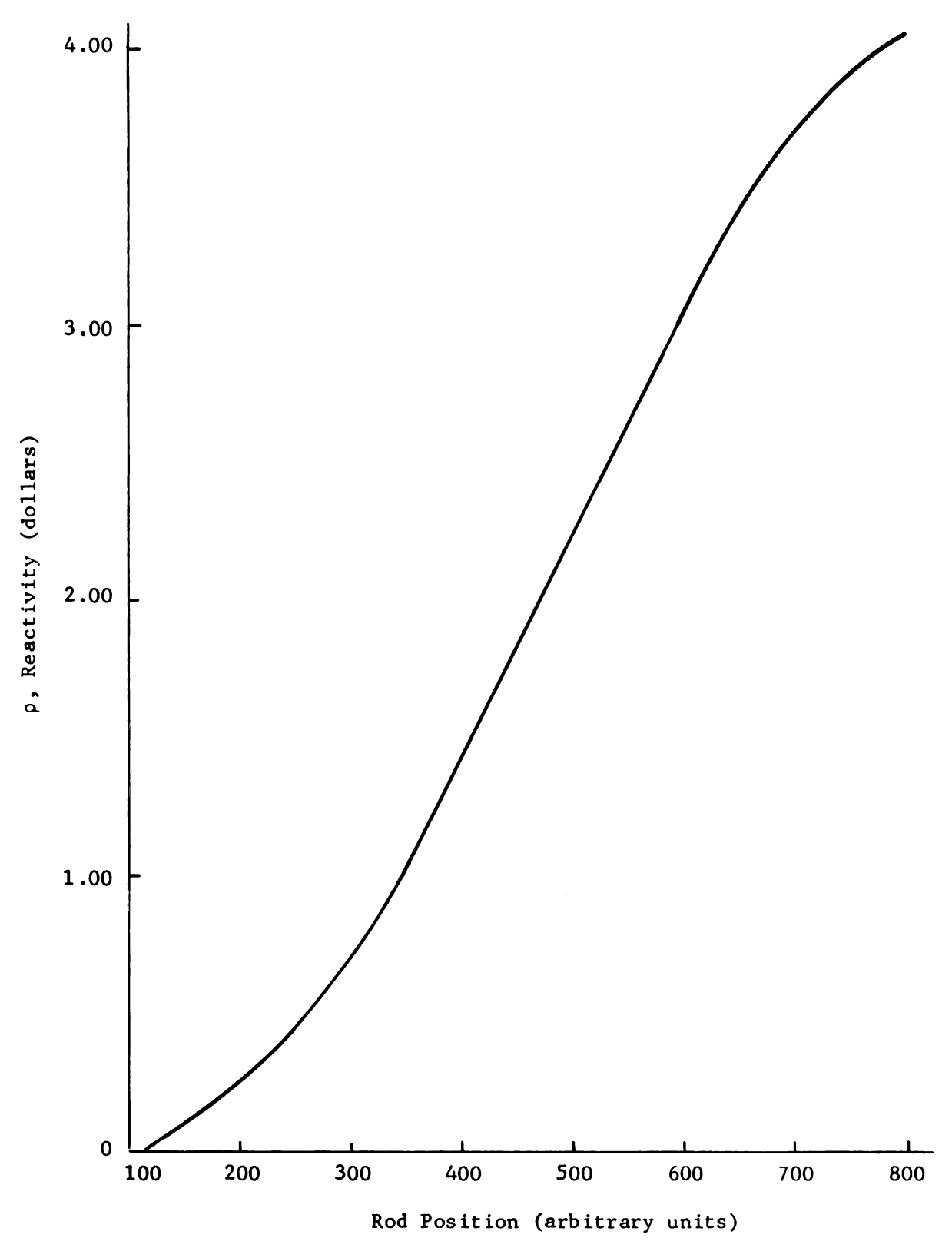


Figure 1.1 Calibration curve for the shim rod in the Michigan State University TRIGA Mark I nuclear reactor

Chapter IV describes a prototype instrument which was built from the design in the previous chapter. Test results and circuit specifications are also given.

Conclusions are made in Chapter V.

CHAPTER II

REACTOR TRANSIENT BEHAVIOR

2.1 Reactivity, Reactor Period and Theoretical Equations

The excess reactivity (hereafter referred to as reactivity)
in a nuclear reactor is defined as the ratio of excess to effective
multiplication factors and is given by

$$\rho = \frac{k_{ex}}{k_{eff}}$$
 (2.1)

In the above formula the effective multiplication factor, $k_{\mbox{eff}} \quad \mbox{is equal to unity for a critical reactor.} \quad \mbox{The excess multiplication factor is}$

$$k_{ex} = k_{eff} - 1 \tag{2.2}$$

and is equal to zero for a critical reactor.

Substitution of Equation (2.2) into Equation (2.1) yields

$$\rho = \frac{\frac{k_{eff} - 1}{k_{eff}}}{k_{eff}}$$
 (2.3)

Since the values of k_{eff} used in this analysis are to be no

The content of this section, except for that material noted otherwise, is taken from M.M. El-Wakil, <u>Nuclear Power Engineering</u> (New York: McGraw-Hill Book Co., 1962), pp. 128-130.

greater than 1.03⁵, Equation (2.3) may be approximated as

$$\rho \cong k_{\text{eff}} - 1 = k_{\text{ex}} \tag{2.4}$$

Using the above approximation for reactivity it is possible to relate $\,\rho\,$ to the instantaneous neutron flux within the reactor.

The equation describing the flux in a supercritical reactor is

$$\Phi = \Phi_0 e^{t/\theta}$$
 (2.5)

The reactor stable period (θ_p) may be written as

$$\theta_{\mathbf{p}} = \frac{\theta_{\mathbf{0}}}{\mathbf{k}_{\mathbf{ex}}} \tag{2.6}$$

and substitution of Equation (2.4) for $k \\ ex \\ relates \\ \rho \\ to \\ \theta \\ p$ where

$$\theta_{\mathbf{p}} \cong \frac{\theta_{\mathbf{0}}}{\rho} \tag{1.2}$$

This approximate expression for θ_p may be substituted into Equation (2.5) to form a relationship between reactor flux and reactivity such that

$$\Phi \cong \Phi_0^{\text{pt/}\theta_0} \tag{2.7}$$

Reference to the rod calibration curve in Figure 1.1 shows the maximum reactivity to be approximately four dollars. This value corresponds to an effective multiplication factor of 1.0292 as defined in the <u>Nuclear Reactor Operations and Training Manuel</u>, <u>Reactor Theory</u> (Michigan State University, 1969), pp. 4-5.

2.2 Relationship Between Reactivity and the Reactor Stable Period

As Equation (1.2) illustrates, the approximate relationship between the reactor stable period and the reactivity is weighted by the mean neutron lifetime. This equation is characterized by a nonlinear property of θ_{n} which is not constant but rather varies slightly with p. Examination of the exact expression for reactivity reveals the source of this nonlinearity. p may be written exactly as

$$\rho = \frac{\theta_0}{\theta_p^{k_{eff}}} + \sum_{i} \frac{\beta_i}{1 + \lambda_i \theta_p}$$
 (2.8)

where β_i is the fraction of delayed fission neutrons in the ith group and λ_i is the respective decay constant.

For large θ_{D} , Equation (2.8) may be approximated as 7

$$\rho \approx \frac{1}{\theta_{p}} \sum_{i} \frac{\beta_{i}}{\lambda_{i}} = \frac{\theta_{0}}{\theta_{p}}$$
 (2.9)

This approximation, however, is only valid for $\theta_{n} > 100$ and as $\theta_{\rm p}$ decreases in value both the first term on the right in Equation (2.8) and the 1 in the denominator of the summation no longer remain negligible. The net effect is a nonlinear relationship between θ_{p} and ρ as illustrated in Figure 2.1.

2.3 Effects of Prompt and Delayed Neutrons on Reactor Transient Behavior

The fission process in the Michigan State University TRIGA Mark I nuclear reactor is described by the following nuclear

Samuel Glasstone, <u>Nuclear Reactor Engineering</u> (New York: D. Van Nostrand Co. Inc., 1963), pp. 244-245.

Ibid., pp. 244-245.

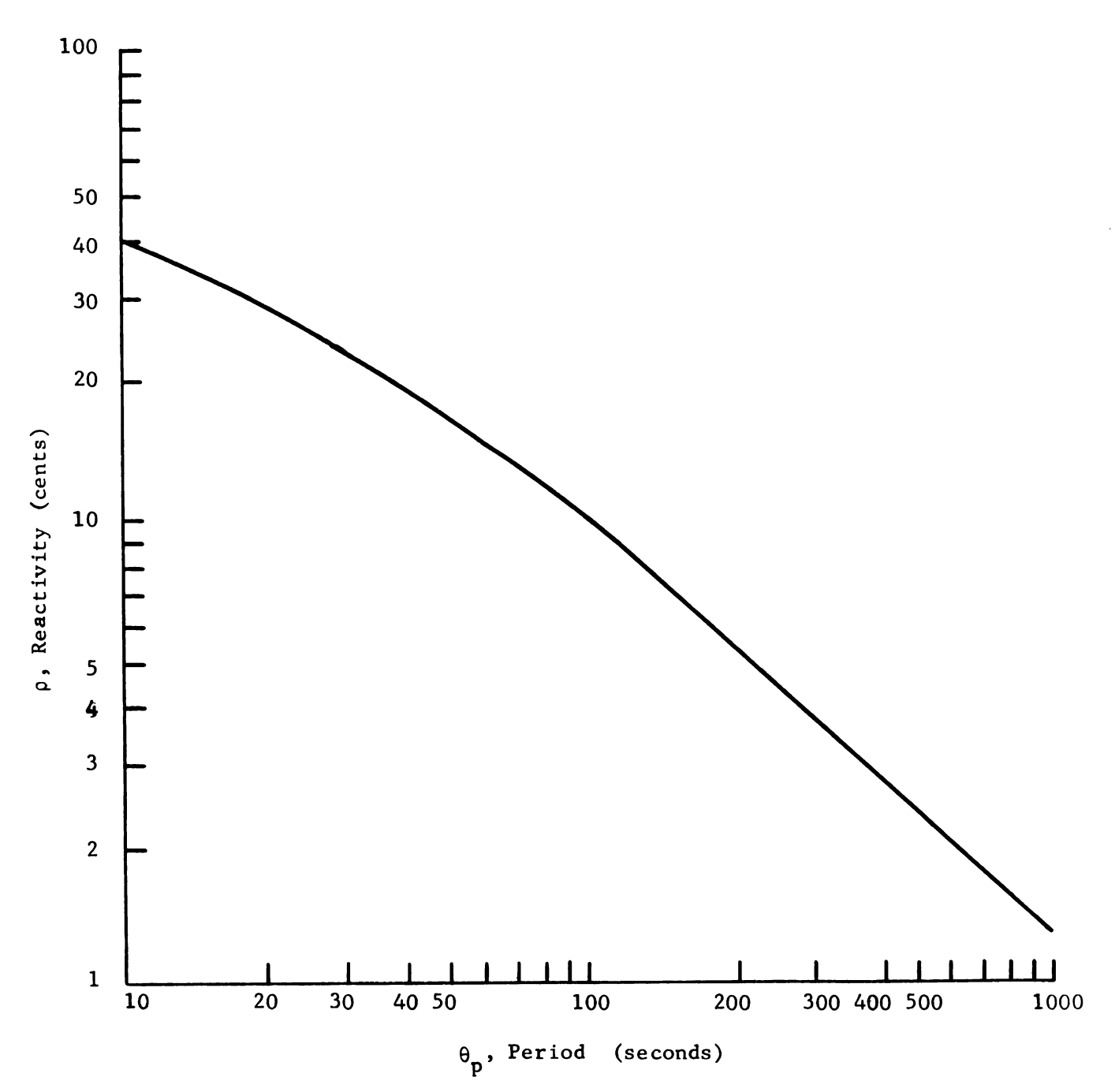


Figure 2.1 Relationship between reactivity and reactor stable period for the Michigan State University TRIGA Mark I nuclear reactor (Courtesy of Gulf General Atomic)

equations:

$$_{92}U^{235} + _{0}n^{1} \rightarrow _{92}U^{236} + energy$$
 (2.10)

or

$$_{92}U^{235} + _{0}n^{1} \rightarrow 2 \text{ fips + energy + } \gamma + c_{0}n^{1}$$
 (2.11)

Equation (2.10) occurs about twenty percent of the time. The fission products (fips) in Equation (2.11) have a variety of atomic weights but will generally weigh about half as much as the U^{235} . Heat is generated by the energy given off in both reactions and the energy is about 200 Mev per fission. On the average between two and three (2 \leq c \leq 3) neutrons are given off per reaction in Equation (2.11). This equation is critical to reactor operation since the neturons produced must sustain the fission chain reaction. 8

Neutrons emitted in Equation (2.11) are of two types:

Prompt neutrons and delayed neutrons. Prompt neutrons make up
about 99.27 percent of all neutrons emitted in the TRIGA reactor.

The total mean lifetime of these prompt neutrons is less than one millisecond.

Delayed neutrons are the result of the decay of certain fission products in Equation (2.11). An example of a delayed neutron emission is given by the nuclear equation

$$53^{137} \xrightarrow{\beta} \begin{array}{c} 34^{137} & n \\ \hline 22 \text{ sec} \end{array} \begin{array}{c} 54^{137} & n \\ \hline \text{instantaneous} \end{array} \begin{array}{c} 54^{136} \\ \end{array}$$
 (2.12)

Training Manuel, Reactor Theory, p. 1.

⁹ Ibid., p. 4.

where $_{53}^{1137}$ is one of the fission products. The 22 second delay in the neutron emission gives it a half life of appearance of 22 seconds. 10

Even though the fraction of delayed neutrons is small, their long apparent lifetimes make the average lifetime of all neutrons emitted much longer than the lifetime of prompt neutrons alone.

This effect is vital since a reactor period caused by prompt neutrons alone would make control of the fission process impossible.

The effect of prompt and delayed neutrons on the change in neutron flux can be described as follows: In a critical reactor withdrawal of a control rod some discrete distance will produce a transient period due to prompt neutrons and a stable period due to the combined effect of prompt and delayed neutrons. The effect of the transient period will result in a "bulge" in the neutron flux. This effect is shown graphically in Figure 2.2. 11

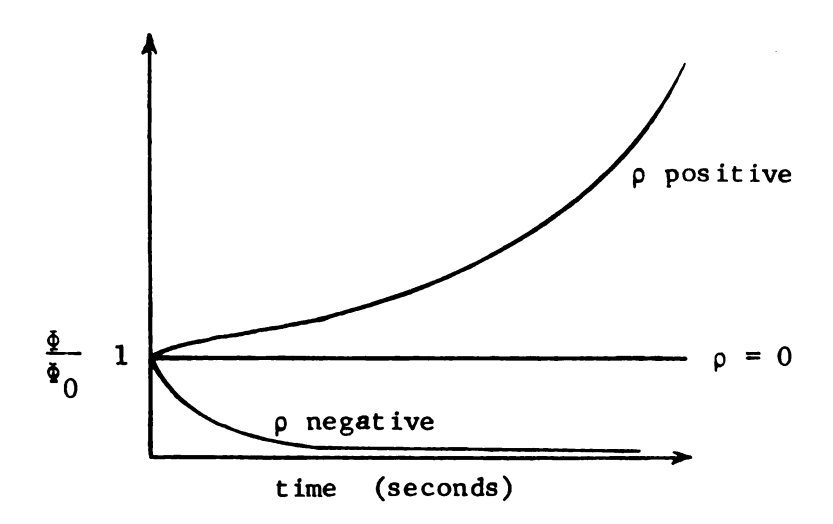


Figure 2.2 Combined effect of prompt and delayed neutrons in a supercritical reactor

E1-Wakil, Nuclear Power Engineering, p. 131.

^{11 &}lt;u>Ibid.</u>, pp. 133-134.

Since ρ is proportional to the slope of the curves in Figure 2.1 it is necessary to let the transient period die out prior to measurement of ρ .

2.4 The Compensated Ion Chamber

It has been stated in Equation (2.7) that the reactivity produced when a discrete portion of control rod is withdrawn from a critical reactor pile is exponentially proportional to the change in neutron flux. In order to measure ρ it is therefore necessary to monitor this flux. This is accomplished in the TRIGA Mark I reactor by means of the output current of a compensated ion chamber located near the reactor core.

The output of the ion chamber is a very low current which is directly proportional to the neutron flux in Equation (2.5) such that

$$i_{s}(t) = I_{0}e^{t/\theta}$$
 (1.1)

where $\theta_{\mathbf{p}}$ may be substituted by the approximate expression

$$\theta_{\mathbf{p}} \cong \frac{\theta_{\mathbf{0}}}{\rho} \tag{1.2}$$

as previously stated.

Figure 2.3 is a simplified diagram of the compensated ion chamber. The device is actually composed of two chambers where $R_{\rm g}$ is the equivalent output resistance. One chamber is lined with boron enriched with B^{10} and is biased at + 580 volts. From this sub-chamber a current proportional to neutron flux and gamma flux is obtained. The other sub-chamber has a variable bias from

0 to -37 volts and is sensitive to gamma flux only. If the gamma sensitive current is subtracted from the gamma, neutron current of the boron coated sub-chamber, a current proportional to neutron flux alone is obtained. 12

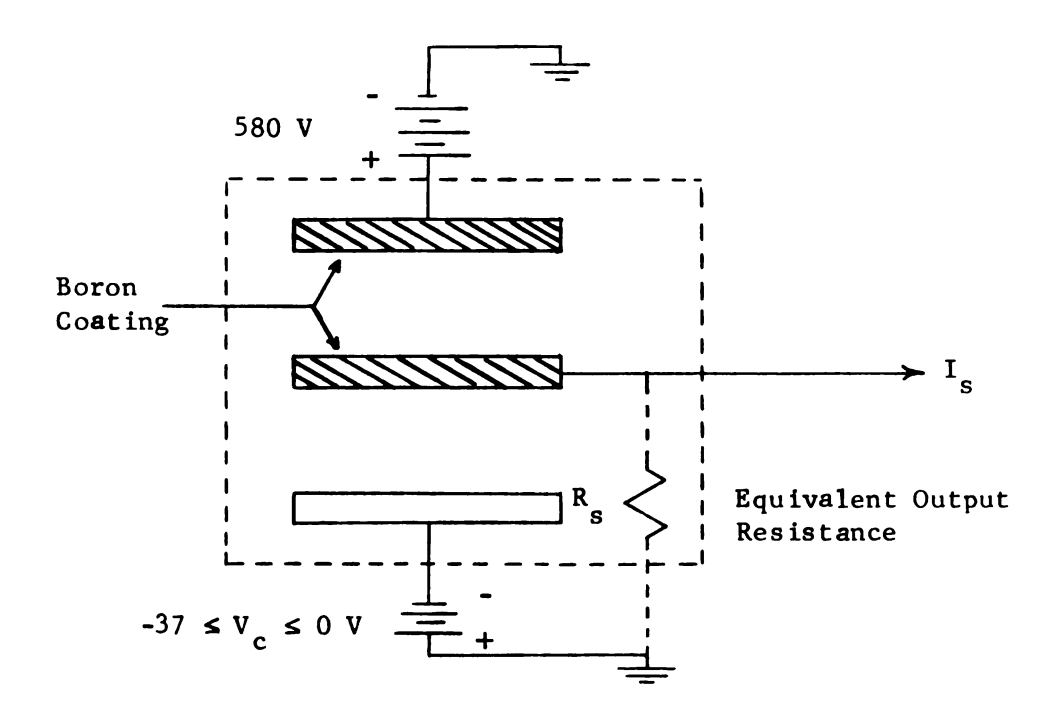


Figure 2.3 Simplified diagram of a compensated ion chamber

At low neutron flux levels ($\phi < 2.5 \times 10^2 \text{n/cm}^2/\text{sec}$), the current contribution from the gamma sensitive chamber is nearly equal to that of the gamma, neutron sensitive chamber. It is therefore important to set the compensating chamber voltage (V_c) to the proper value in order to achieve a linear response due to neutron flux alone. This leaves room for error in the linearity of $i_s(t)$ if V_c is not properly adjusted. Fortunately, as the neutron flux level increases the current contribution to $i_s(t)$

¹² Training Manuel, Instrumentation, p. 5.

due to gamma flux alone becomes negligible and i (t) approaches a linear dependance on neutron flux alone.

Experimental results reveal that improper adjustment of the compensating voltage at low reactor flux levels (corresponding to reactor output power levels below ten watts) causes the output current of the ion chamber (i_s(t)) to become nonlinear. Figure 2.4 shows the maximum nonlinear effects at low power levels when the compensating voltage is adjusted to zero volts.

Since a linear relationship between ion chamber current (ig(t)) and neutron flux (also reactor output power level) is necessary, it is best to rely only upon output currents which correspond to reactor power levels greater than ten watts.

Specifications of the ion chamber are given in Appendix E. Since the output resistance is greater than 10^{13} ohms, the chamber may be considered as a current source.

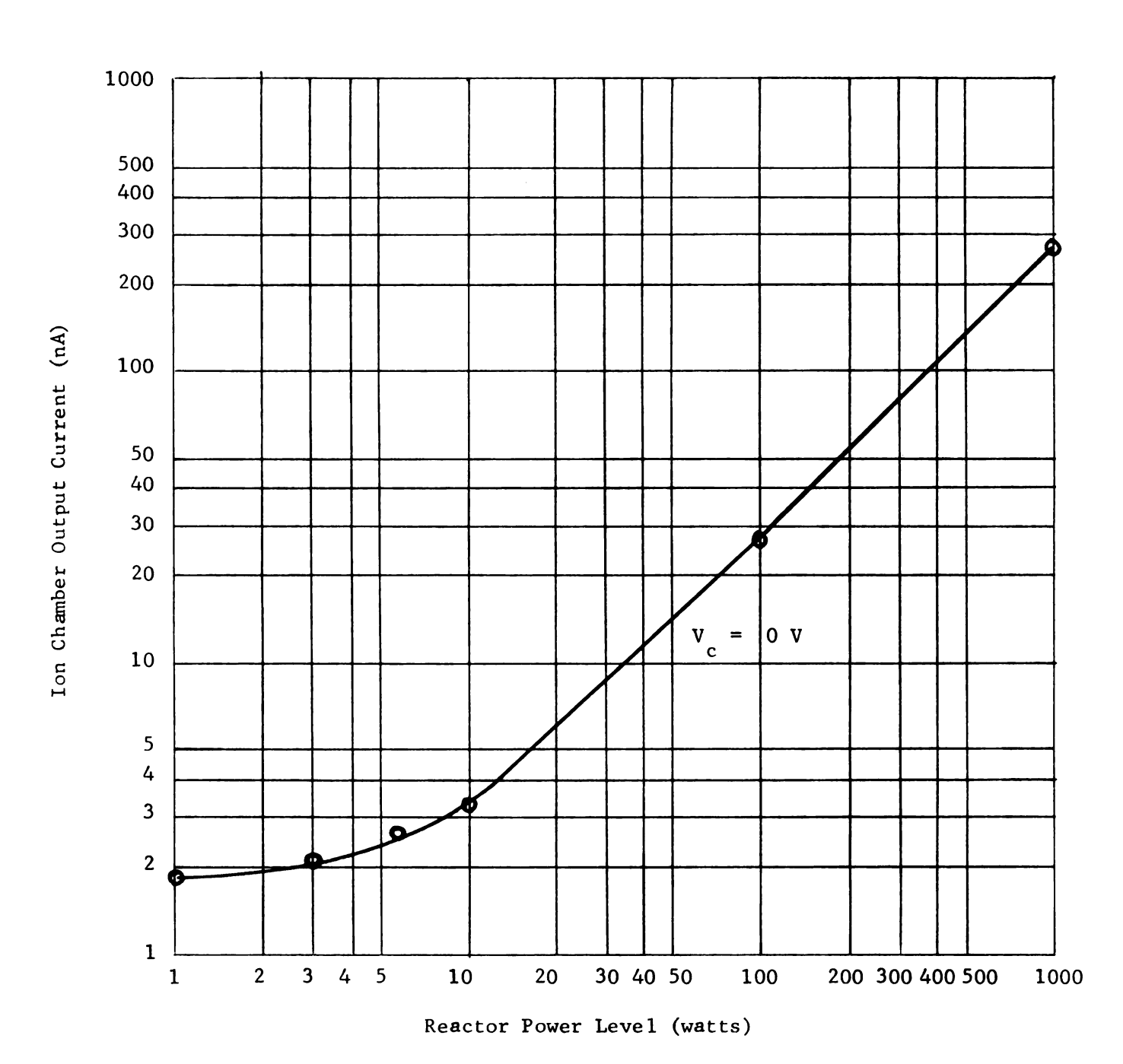


Figure 2.4 Graph of ion chamber output current as a function of output power level for the Michigan State University TRIGA Mark I nuclear reactor

CHAPTER III

DESIGN OF THE REACTIVITY MEASURING DEVICE

3.1 Formulation of the Problem

Having presented the equations defining reactivity and its relationship to the output current of the ion chamber it now remains to develop a means by which $\,\rho\,$ can be measured.

$$i_s(t) = I_0 e^{t/\theta} p$$
 (1.1)

The objective is to process this current so as to produce a voltage proportional to the reactor stable period. If this can be accomplished effectively then θ_p may be related to ρ as in Equation (1.2) since

$$\theta_{\mathbf{p}} \cong \frac{\theta_{\mathbf{0}}}{\rho} \tag{1.2}$$

Because this relationship is slightly nonlinear as the graph in Figure 2.2 illustrates, the value of ρ corresponding to a given θ_p may be taken from this graph and used to calibrate the reactivity meter.

3.2 Possible Methods of Solution 13

Given the desired output $\,\rho\,$ and the input $\,i_{\,\,s}(t)\,$ several methods for determining $\,\rho\,$ will now be considered.

One method makes use of the circuit in Figure 3.1 where a d-c voltage proportional to $1/\theta_p$ is obtained from $i_s(t)$ using a logarithmic amplifier followed by a differentiator and filter.

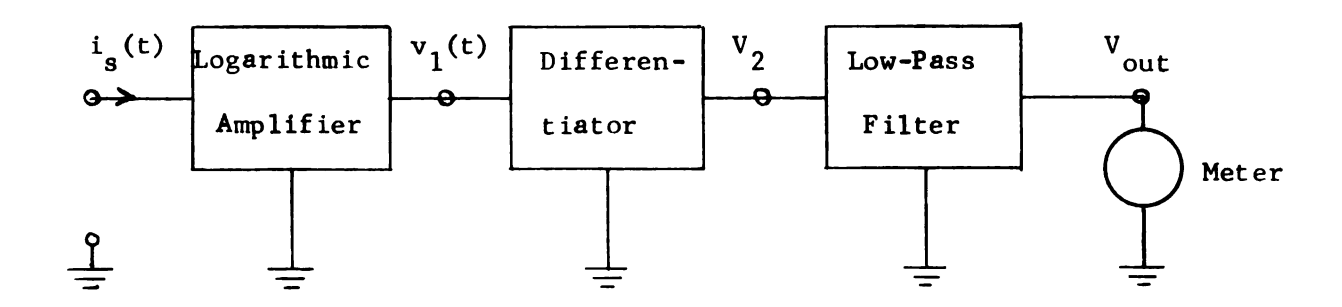


Figure 3.1 Block diagram of a circuit which provides a d-c voltage proportional to the inverse of the reactor stable period

In a circuit of this type the logarithm of the ion chamber current is first taken such that

$$v_1(t) = -A \log_{10} i_s(t) = -A \log_{10} I_0 e^{t/\theta_p} = -A \log_{10} I_0 - \frac{At}{\theta_p} \log_{10} e$$
 (3.1)

The voltage $v_1(t)$ is a linear ramp function whose slope is inversely proportional to the negative inverse of θ_p . Differentiation of this ramp voltage yields a d-c voltage V_2 where

$$V_2 = \frac{-Kd}{dt} V_1(t) = \frac{-Kd}{dt} (-A \log_{10} I_0 \frac{At}{\theta_p} \log_{10} e) = \frac{KA}{\theta_p} \log_{10} e$$
 (3.2)

The first two methods presented were suggested by Dr. L. Giacoletto of Michigan State University. The third method was developed by the author.

The result is a d-c voltage inversely proportional to θ_p . This voltage is then passed through a low-pass filter to eliminate any low-frequency noise components passed by the differentiator.

Finally, due to the slight nonlinear relationship between θ_p and ρ the voltage V_{out} (Figure 3.1) is calibrated on a meter via Figure 3.6 to indicate exact values of reactivity.

A second method for obtaining a d-c voltage proportional to θ_p involves the use of an integrator and a quarter-square multiplier. The circuit is pictured in Figure 3.2.

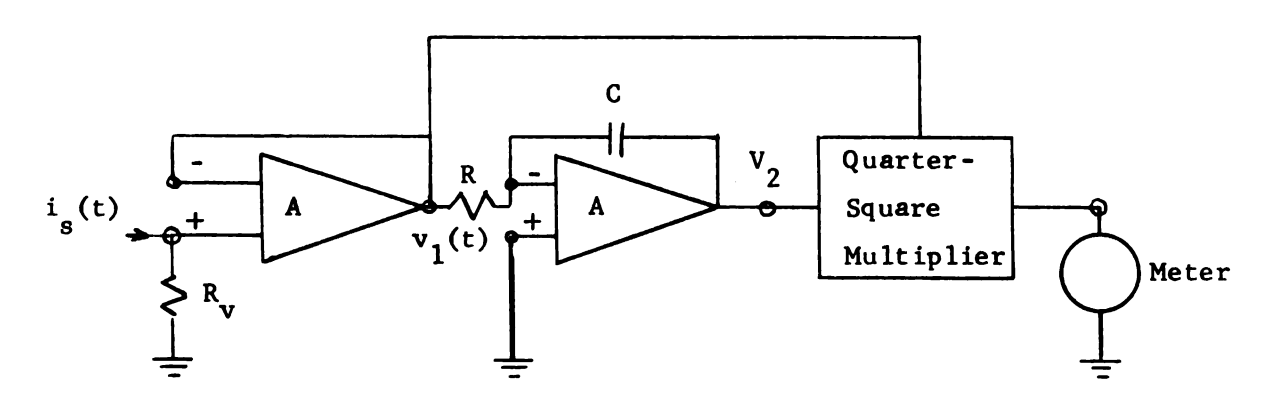


Figure 3.2 Circuit for obtaining a d-c voltage proportional to θ_p

In this circuit the input current $(i_s(t))$ is first converted to a voltage

$$v_1(t) = i_s(t)R_v = I_0R_v e^{t/\theta}$$
 (3.3)

using a buffer amplifier whose input resistance is much greater than $\,R_{_{\rm \! V}}^{}.$

This voltage is then integrated to obtain $v_2(t)$ where

$$v_2(t) = \frac{-1}{RC} \int_0^t v_1(t) dt = \frac{-I_0^R v_p^{\theta}}{RC} (e^{t/\theta} - 1)$$
 (3.4)

The quarter-square multiplier is next used to divide out the exponential term in $v_{\gamma}(t)$ such that

$$v_{\text{out}} = \frac{v_2(t)}{v_1(t)} = \frac{-I_0 R_v \theta_p}{RC} (e^{t/\theta_p} - 1) \frac{1}{I_0 R_v e} \approx \frac{-\theta_p}{RC}$$
 (3.5)

This resultant d-c voltage is proportional to θ_p and can therefore be calibrated on a meter using the graph of Figure 3.6 to represent the corresponding values of reactivity.

A third method for finding θ_p involves the integration of a voltage proportional to the change of the input current. Figure 3.3 is a simplified diagram of the circuit.

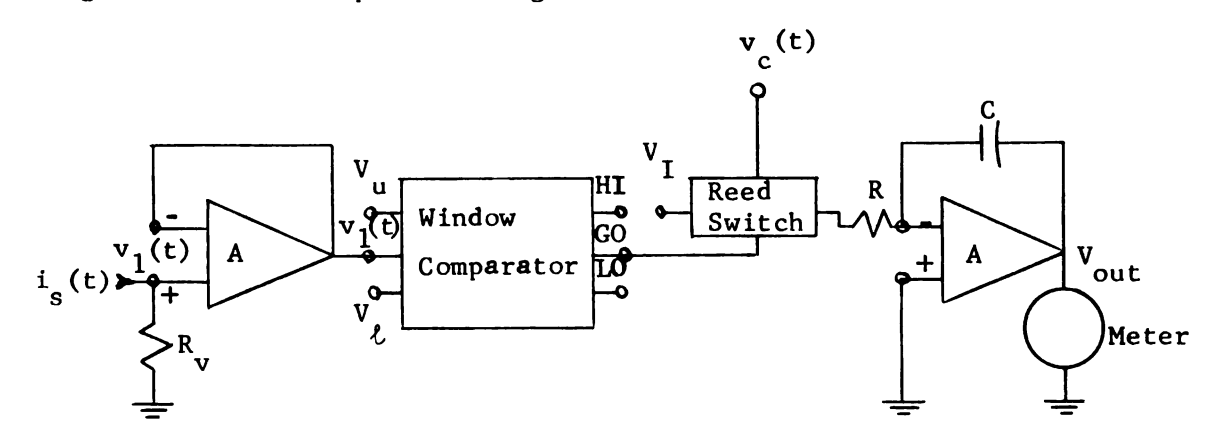


Figure 3.3 Circuit for obtaining a discrete voltage proportional to the slope of $i_s(t)$

The input current is first converted to a voltage $v_1(t)$ such that

$$v_1(t) = i_s(t)R_v = I_0R_v e^{t/\theta}$$
 (3.3)

This voltage is then fed into a window comparator whose "GO" output (Figure 3.3) acts as a current sink for $V_{\ell} \leq v_1(t) \leq V_{u}$ and as a large resistance whenever $v_1(t) < V_{\ell}$ or $v_1(t) > V_{u}$. The "GO" condition will allow the current $i_c(t)$ to flow in the coil

of the reed switch and close its contacts. When this occurs the d-c voltage V_{I} is switched to the input of the integrator and is integrated for the period of time that $v_{I}(t)$ remains within the bounds of V_{u} and V_{ℓ} . This period of time is proportional to θ_{p} and is also proportional to the final integrator output voltage. The relationship between V_{out} and θ_{p} can be found by starting with the output voltage integral

$$v_{out} = \frac{-1}{RC} \int_{0}^{\theta_{t}} v_{I} dt$$
 (3.6)

The total integration time (θ_t) is that period of time that $V_{\ell} \leq v_1(t) \leq V_u$ and may be calculated by substituting V_u and V_{ℓ} into the equation for $v_1(t)$ where

$$v_1(\theta_L) = V_L = R_{\mathbf{v}} I_0 e^{\theta_L / \theta_p}$$
(3.7)

and

$$\mathbf{v}_{1}(\theta_{1}) = \mathbf{v}_{1} = \mathbf{R}_{1}\mathbf{I}_{0}e^{\theta_{1}/\theta_{p}}$$
(3.8)

 $\theta_{\boldsymbol{\ell}}$ and θ_{u} are the times for which $\boldsymbol{v}_{1}(t)$ is equal to \boldsymbol{v}_{ℓ} and \boldsymbol{v}_{u} respectively.

Equations (3.7) and (3.8) are then solved for the time increment θ_t where $\theta_t = \theta_u - \theta_t$ and

$$\theta_{t} = \theta_{u} - \theta_{\ell} = \theta_{p} (\ln \frac{v_{u}}{R_{v}I_{0}} - \ln \frac{v_{\ell}}{R_{v}I_{0}})$$
 (3.9)

Using Equation (3.9) for the value of θ_t in the integral of Equation (3.6), the voltage V_{out} may be written as

$$V_{\text{out}} = \frac{-1}{RC} \theta_{p} (\ln \frac{V_{u}}{R_{v}I_{0}} - \ln \frac{V_{\ell}}{R_{v}I_{0}})$$
 (3.10)

which is a d-c voltage proportional to the stable reactor period.

As in the first two methods this voltage may be calibrated on a meter using the nonlinear graphical relationship of Figure 3.6 to indicate the corresponding value of reactivity.

The above method for measurement of reactivity differs from the preceeding two in that the output voltage is not a continuous representation of θ_p but rather a discrete value obtained after integrating a d-c voltage over a discrete time period θ_t .

After consideration of the three alternatives the method chosen to measure ρ was the first one described using a logarithmic amplifier followed by a differentiator and filter (Figure 3.1).

3.3 The Circuit and Theory of Operation

With the reactivity measurement solution method chosen, the circuit of Figure 3.4 was designed to produce a d-c voltage proportional to θ_n .

The transfer function of the circuit is

$$V_{\text{out}} = V_1(s) \frac{(-R_2C_1s)}{(R_1C_1s+1)(R_2C_2s+1)} \frac{1}{(R_fC_fs+1)}$$
 (3.11)

where V_1 (s) is the frequency domain expression for v_1 (t) given as

$$v_{1}(s) = \frac{-A \log_{10}(I_{0}/I_{k})}{s} - \frac{A \log_{10}e}{\theta_{p}s^{2}}$$
(3.12)

and A is the logarithmic amplifier voltage constant determined approximately by

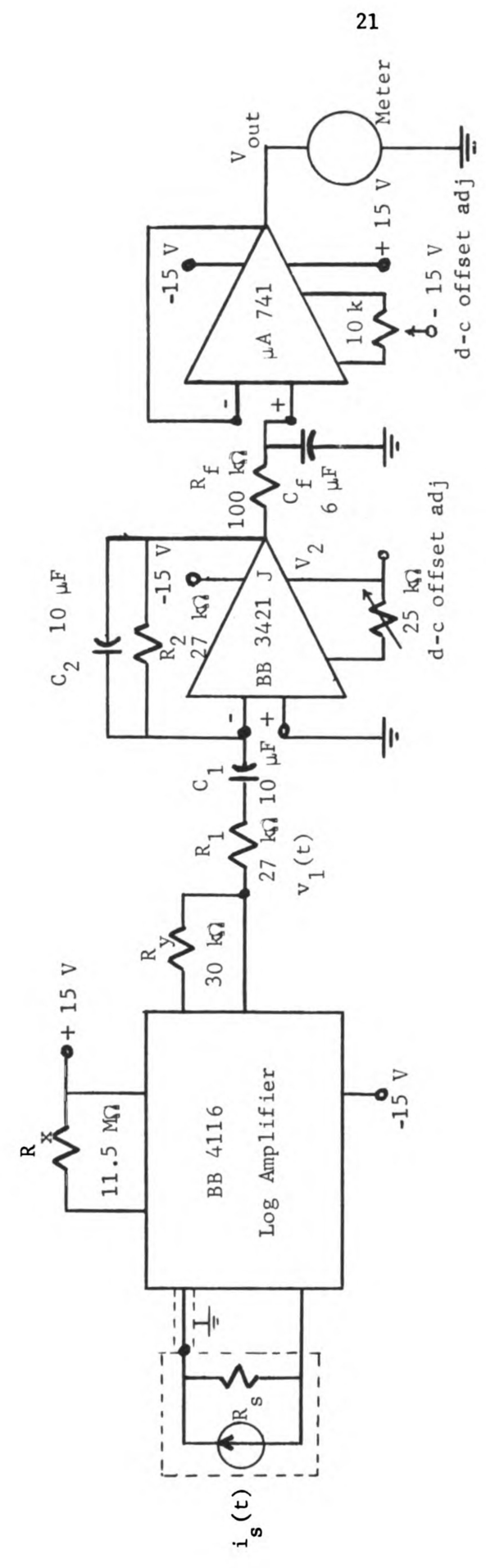


Figure 3.4 Circuit diagram of the reactivity measuring instrument

Power Supply: Calex model 22-100

$$A \simeq \left(\frac{R_y + 5000 + R_3}{R_3}\right) \frac{(26 \times 10^{-3})}{.434} \text{ Volts}$$
 (3.13)

where R₃ is a temperature dependant resistor within the logarithmic amplifier module. 14

 $\rm I_k$ is the log amplifier reference current determined primarily by $\rm\,R_x^{.15}$

The concept by which the circuit works is as follows: Using the ion chamber current as the input, the logarithm of $i_s(t)$ is first taken. The output voltage $(v_1(t))$ is a linear ramp function since

$$v_{1}(t) = -A \log_{10} \frac{i_{s}(t)}{I_{k}} = -A \log_{10} (\frac{I_{0}}{I_{k}} e^{t/\theta})$$

$$= -A \log_{10} \frac{I_{0}}{I_{k}} - \frac{At}{\theta_{p}} \log_{10} e$$
(3.14)

 $v_1^{(t)}$ is then differentiated to produce a d-c voltage $v_2^{(t)}$ where

$$G_{\theta_{t}}(t - \theta_{t/2}) = 1 \quad 0 \le t \le \theta_{t}$$

$$G_{\theta_{t}}(t - \theta_{t/2}) = 0 \quad t < 0, t > \theta_{t}$$

Modular Logarithmic Amplifier Model 4116 (Burr-Brown Research Corp., 1971), p.3.

A more complete discription of the logarithmic amplifier and its parameters is given in Appendix A.

Since the input current $(i_s(t))$ is an exponentially increasing function and since the circuit (Figure 3.4) used to process this function has a limit to the absolute magnitude of the input, $i_s(t)$ can only remain "on" for a discrete period of time θ_t . Therefore, in order to be absolutely correct when defining $i_s(t)$ the gate function notation should be used where

 $[\]theta_{t}$ is the time of the input pulse. Using this notation $i_{s}(t)$ becomes

$$v_{2} = -R_{2}C_{1} \frac{d}{dt} v_{1}(t) = -R_{2}C_{1} \frac{d}{dt}(-A \log_{10} \frac{I_{0}}{I_{k}} - \frac{At}{\theta_{p}} \log_{10} e)$$

$$= \frac{R_{2}C_{1}A}{\theta_{p}} \log_{10} e$$
(3.15)

This d-c voltage is then filtered to eliminate any low-frequency noise enhanced by the differentiator. The resultant voltage V_{out} is inversely proportional to the reactor stable period and approximately proportional to the reactivity such that

$$V_{\text{out}} = \frac{R_2 C_1^A}{\theta_p} \log_{10} e \cong \rho \frac{R_2 C_1^A}{\theta_0} \log_{10} e$$
 (3.16)

As previously discussed (Section 2.2) the relationship between θ_p and ρ is nonlinear. Calibration of the meter may be accomplished by producing known reactor periods and marking the meter deflection with the corresponding values of ρ via the graph in Figure 3.6.

A comprehensive analysis of the circuit design is given in Appendices A, B, C and D.

3.4 Calibration

The output voltage in the circuit of Figure 3.4 is a d-c voltage proportional to the inverse of $\theta_{\rm p}$ and approximately

$$i_s(t) = I_0 e^{t/\theta} p \left[G_{\theta_t}(t - \theta_{t/2}) \right]$$

If the gate function notation is carried with $i_s(t)$ two finite strength impulses will appear when $v_1(t)$ is differentiated in Equation (3.15) due to differentiation of the gate function.

Although these finite strength impulses are of importance (particularly since they show up on the output when $i_s(t)$ is switched on and off) they shall not be carried in the analysis. It should be understood, however, that $i_s(t)$ is on for a finite period of time. This period of time (θ_t) is discussed further in Appendix B.

proportional to ρ where

$$V_{\text{out}} = \frac{R_2 C_1 A}{\theta_p} \log_{10} e^{-\frac{R_2 C_1 A}{\theta_0}} \log_{10} e^{-\frac{R_2 C_1 A}{\theta_0}}$$

As previously mentioned the relationship between θ_p and ρ is nonlinear. Figure 3.6 illustrates this relationship for the Michigan State University TRIGA Mark I reactor.

The range of reactor stable periods for which the meter is to be calibrated is 10 sec $\leq \theta_p \leq 40$ sec. This range corresponds to a range of reactivity between 40 and 19 cents respectively. (Figure 3.6)

Calibration of the reactivity meter is accomplished with the apparatus in Figure 3.5.

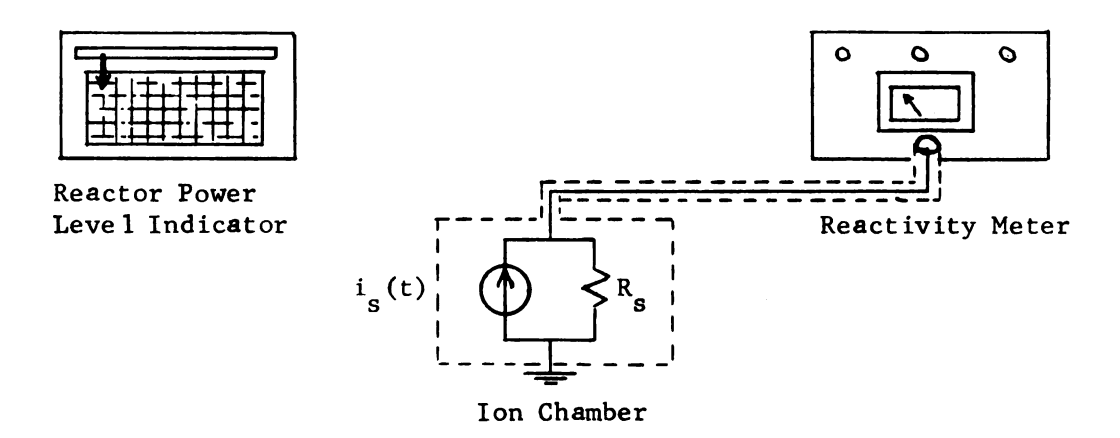


Figure 3.5 Apparatus used to calibrate the reactivity meter

The reactor is first made critical with the ion chamber current equal to $\ I_0$. A control rod is then pulled out a discrete distance and the ion chamber current becomes

$$i_s(t) = I_0 e^{t/\theta}$$
 (1.1)

The corresponding d-c voltage on the reactivity meter will be

$$v_{out} = \frac{R_2^C_1^A}{\theta_p} \log_{10}^A e$$
 (3.16)

This voltage is then marked on the meter.

In order to mark the reactivity corresponding to $V_{\rm out}$ the graph of Figure 3.6 is used. As this graph indicates the reactor stable period must be known. This value is determined by using the reactor power level indicator and a timer to find the power level doubling time θ_d . The period can be calculated from the doubling time since

$$\theta_{p} = \frac{\theta_{d}}{\ln 2} \tag{3.17}$$

This process is repeated until the range of $\,\rho\,$ is adequately covered.

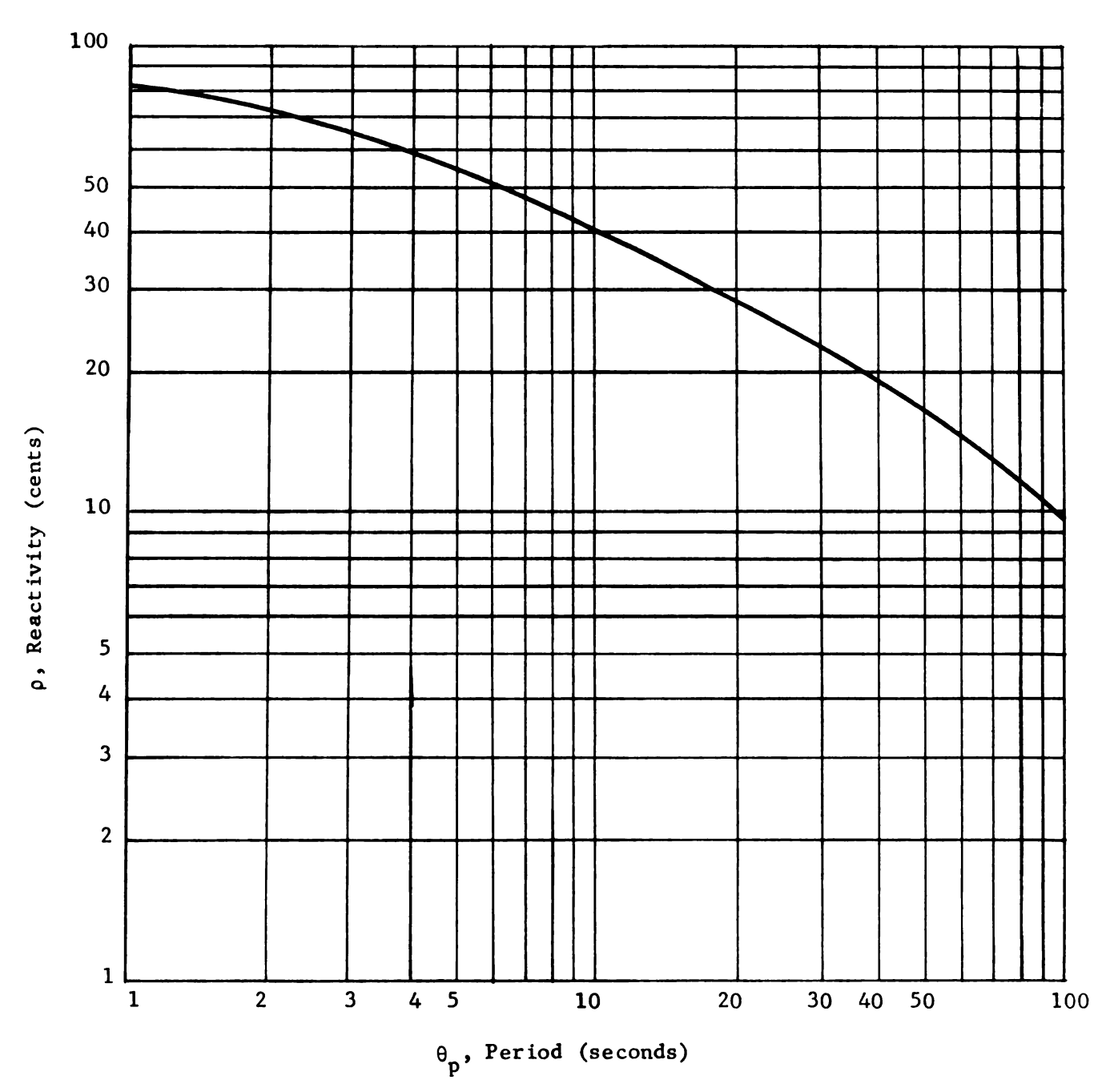


Figure 3.6 Graph showing the relationship between reactivity and reactor stable period for the Michigan State University TRIGA Mark I nuclear reactor (Courtesy of Gulf General Atomic)

CHAPTER IV

CONSTRUCTION OF THE REACTIVITY METER

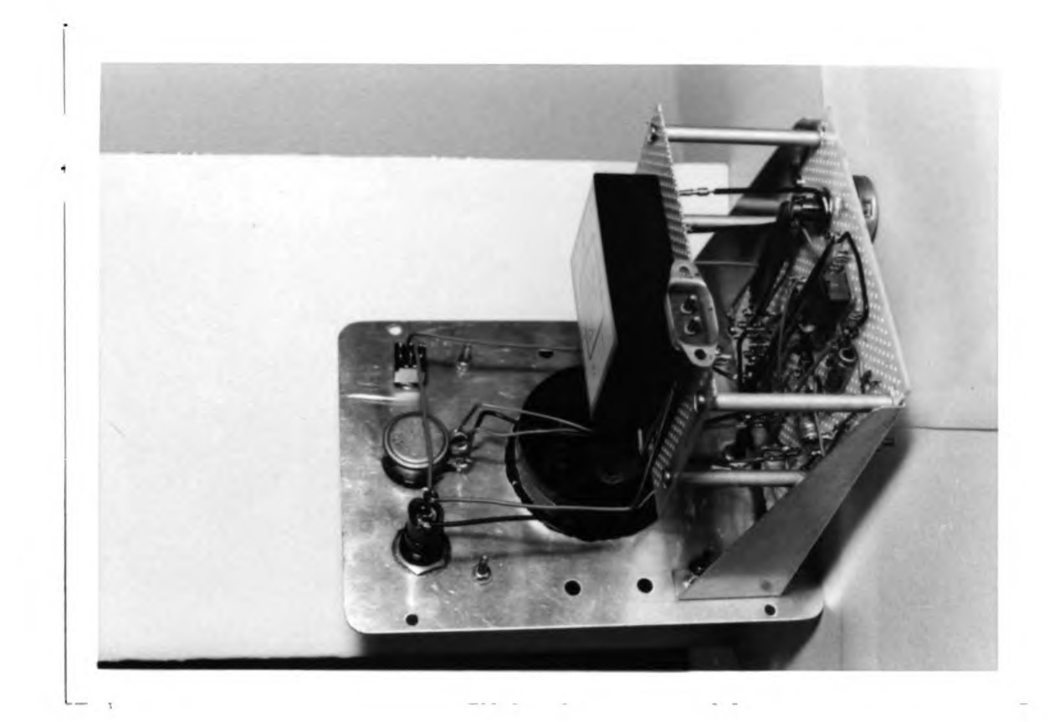
4.1 Circuit Tests, Performance and Specifications

The circuit of Figure 3.4 was constructed and tested. Figure 4.1 shows several photographs of the instrument.

Testing of the circuit was accomplished by connecting the meter input to the ion chamber via a coaxial cable. The reactor was then made critical and a control rod withdrawn to produce a reactor period within the desired range. The range of the meter was checked for consistancy and variation due to noise. These tests revealed the meter deflection to be approximately 77 percent for a 10 second period and approximately 24 percent for a 40 second period thus adequately covering the desired range of θ_p . The maximum variation in meter reading due to noise was less than \pm 0.4 percent of full scale.

The minimum reactor power level for which the circuit was designed to operate is ten watts. This corresponds to an ion chamber current, $I_0 = 3nA$. Values of input current below this level will put the logarithmic amplifier in saturation and therefore cause V_{out} to register inaccurately on the meter.

The upper power level was chosen to be 200 watts resulting in an ion chamber current of 60 nA. This value is not an absolute upper limit and the meter will continue to read accurately up to



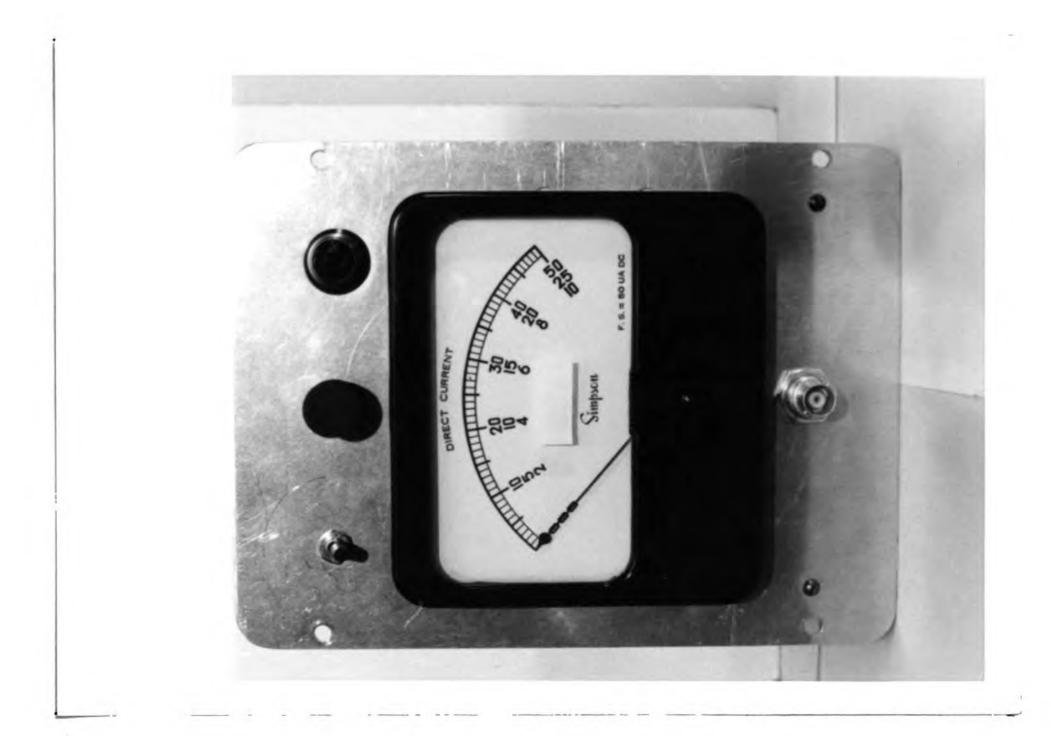


Figure 4.1 Photographs of the reactivity meter

a reactor power level of 1000 watts ($i_8(t) = 280$ na) at which time the negative temperature coefficient inherent in the reactor will cause the meter to lose accuracy.

The final specifications of the reactivity meter are listed in Table 4.1.

Table 4.1 Specifications of the reactivity meter

Input: Exponentially increasing current $i_s(t) = I_0^{e}$
θ _{p min} 10 seconds
θ max 40 seconds
I 3 × 10 ⁻⁹ Amperes
I 60 × 10 ⁻⁹ Amperes
Output reactivity (ρ) in cents
ρ _{min} 19 cents
ρ _{max} 40 cents
Accuracy (after calibration) ± 0.5 percent

Since the values of ρ on the meter are calibrated from a graph, the only error will be that variation caused by noise on the output voltage of the filter (Figure 3.4).

CHAPTER V

CONCLUSIONS

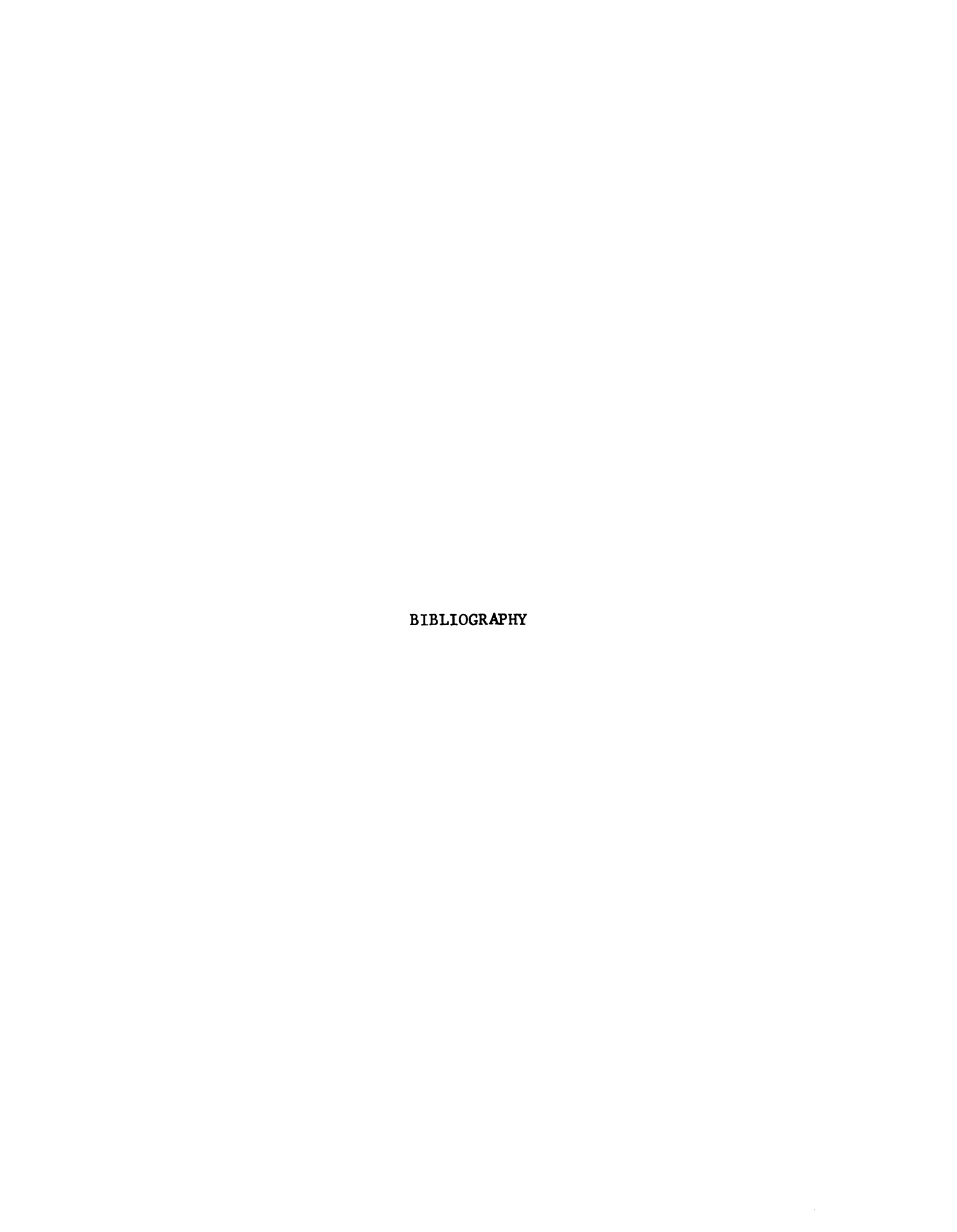
The control rod calibration curve in Figure 1.1 is of the type for which the reactivity meter was designed to produced.

Original design specifications called for the measurement of periods between 10 and 40 seconds corresponding to reactivities between 40 and 19 cents. As the graph indicates, these values cover only a small portion of the total rod calibration curve.

In order to cover the entire range of the calibration curve the measured values of rod reactivity must be added in increments within the range of the meter. For example: Reference to the graph of Figure 1.1 shows the reactivity corresponding to a rod position of 300 to be approximately 60 cents. If at this position the reactor were made critical and the rod pulled out to a position of 350, a reactivity of about 40 cents would be recorded on the meter. In order to get the total rod worth at this new position this value of reactivity would have to be added to the previous total reactivity of 60 cents and would therefore yield the new total reactivity of approximately 1 dollar.

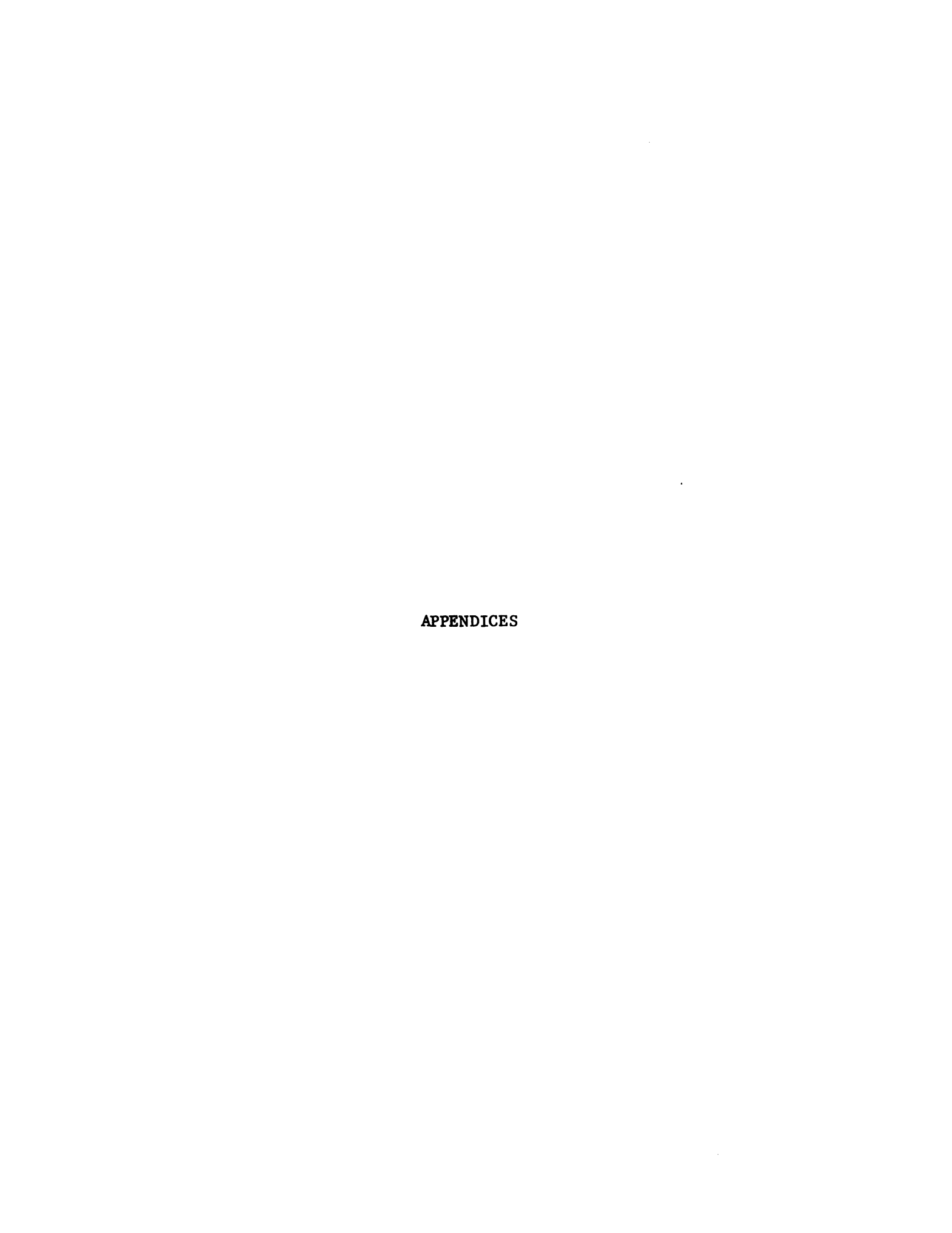
It should also be noted that since the total rod worth is determined by the sum of incremental reactivities the error in measurement of each incremental rod worth becomes very important and the total error increases with each sum.

The overall results of the tests made on the instrument reveal that the reactivity meter works well for the range of input currents and reactor periods for which is was designed.



BIBLIOGRAPHY

- E1-Wakil, M.M. <u>Nuclear Power Engineering</u>. New York: McGraw-Hill Book Co., 1962.
- Glasstone, Samuèl. <u>Nuclear Reactor Engineering</u>. New York: D. Van Nostrand Co. Inc., 1963.
- Jackson, Albert S. Analog Computation. New York: McGraw-Hill Book Co., 1960.
- Modular Logarithmic Amplifier Model 4116. Burr-Brown Research Corp., 1971.
- Nuclear Reactor Operations and Training Manuel. Michigan State University, 1969.
- RCA Linear Integrated Circuits. RCA, 1967.
- Selby, Samuel M. <u>CRC Standard Mathematical Tables</u>. Cleveland, Ohio: The Chemical Rubber Co., 1965.
- Westinghouse WL-8105. New York: Westinghouse Electric Co., 1965.



APPENDIX A DESIGN OF THE LOGARITHMIC AMPLIFIER

APPENDIX A

DESIGN OF THE LOGARITHMIC AMPLIFIER 17

The logarithmic amplifier used in constructing the circuit of Figure 3.4 is a Burr-Brown model 4116 modular logarithmic amplifier. Its purpose in the circuit is to take the logarithm of the input current i (t) where

$$i_{s}(t) = I_{0}e^{t/\theta}$$
 (1.1)

The resultant output is a linear ramp function given by

$$v_{1}(t) = -A \log_{10} \frac{i_{s}(t)}{I_{k}} = -A \log_{10} \frac{I_{0}}{I_{k}} e^{t/\theta_{p}}$$

$$= -A \log_{10} \frac{I_{0}}{I_{k}} - \frac{At}{\theta_{p}} \log_{10} e$$
(3.14)

There are two design parameters for this amplifier. These are the voltage scale factor A and the reference current $\mathbf{I_k}$. Figure A.1 shows the logarithmic amplifier with exterior connections. The electrical specifications are given in Table A.1.

The design equations, graphs, figures and specifications in this section were taken from the pamphlet Modular Logarithmic Amplifier Model 4116 (Burr-Brown Research Corp., 1971), pp. 1-5.

Table A.1 Electrical specifications of the Burr-Brown modular logarithmic amplifier model 4116 (current input only)

Accuracy
Accuracy, percent of full scale with current source input for $0.4nA \le I_S \le 400 \mu A \dots \pm 1$ percent
<u>Input</u>
Current Source Input
Absolute Maximum Current ± 10 mA
Reference Current Range (I_k)
Voltage Scale Factor Range (A) $2/3 \text{ V} \leq A \leq 10 \text{ V}$
<u>Output</u>
Current <u>+</u> 5 mA
Voltage <u>+</u> 10 V
Output Impedance at A = 5
<u>Stability</u>
Scale Factor Drift (△A/°C) ± 0.0005 A/°C
Reference Current Drift $(\Delta I_k/^{\circ}C)$
for 0.4 μ A $\leq I_k \leq 1 \mu$ A $\pm 0.003 I_k$ /°C
Input Offset Current Drift $(\Delta I_s/^{\circ}C)10$ pA at $25^{\circ}C$, 1 pA/ $^{\circ}C$
Input Noise - Current Input 1 pA rms, 10 Hz. to 10k Hz.
Power Supply
Rated Voltage ± 15 Vdc
Supply Drain (Quiescent) ± 22 mA

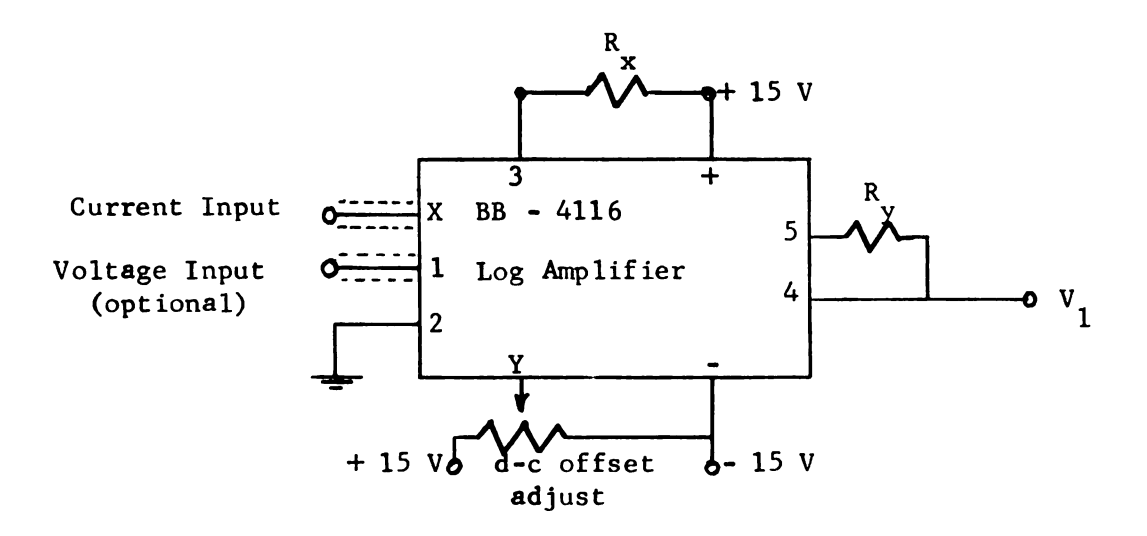


Figure A.1 Burr-Brown modular logarithmic amplifier model 4116 with external connections

A design that takes advantage of the full range of output voltage is best. The values of $R_{\mathbf{x}}$ and $R_{\mathbf{y}}$ required to accomplish this may be obtained by first solving Equation (3.14) for the full \pm 10 volt range where

$$V_{1 \text{ max}} = -A \log_{10} \frac{I_{\min}}{I_{k}} = 10 \text{ Volts}$$
 (A.1)

$$V_{1 \text{ min}} = -A \log_{10} \frac{I_{\text{max}}}{I_{k}} = -10 \text{ Volts}$$
 (A.2)

These equations may be added to solve for $\ensuremath{\mathrm{I}}_k$ with the result

$$I_{k} = (I_{max} I_{min})^{\frac{1}{2}}$$
 (A.3)

The corresponding voltage scale factor (A) may next be found by substitution of Equation (A.3) into Equation (A.1) for I_k . This provides an expression for A where

$$A = \frac{10}{\log_{10} \left(\frac{I_{\text{max}}}{I_{\text{min}}}\right)^{\frac{1}{2}}}$$
 (A.4)

In Chapter IV it was established that the value of I_{min} would be 3nA and I_{max} would be 60nA. Substitution of these values into the expressions for I_k and A yields

$$I_{L} = 12.96 \text{ nA}$$
 (A.5)

$$A = 15.75 \text{ Volts} \tag{A.6}$$

At this point a problem is encountered. Figure A.2 shows the graphical relationships between I_k , A and their design resistors. Reference to these graphs and to the specifications in Table A.1 indicate that the values of I_k and A in Equations (A.5) and (A.6) are outside the design limits.

A compromise must be made to reduce the output voltage range in order to put I_k and A within their respective tolerances. For the final design a value of $R_{_{\rm X}}$ = 11.3 MN was selected. This corresponds to a reference current of .564A.

Using this value for I_k the best value for A can be calculated by letting the output be 10 volts for $I_{s\ min}$. Substitution into Equation (A.1) yields

$$A = \frac{-10}{\log_{10} \frac{I_{\min}}{I_k}} = \frac{-10}{\log_{10} \frac{3 \times 10^{-9}}{.56 \times 10^{-6}}} = 4.5$$
 (A.7)

Reference to the graph in Figure A.2b indicates a value of 28 k Ω for R will make A equal to 4.5 volts.

The actual output range of the logarithmic amplifier may now be calculated where

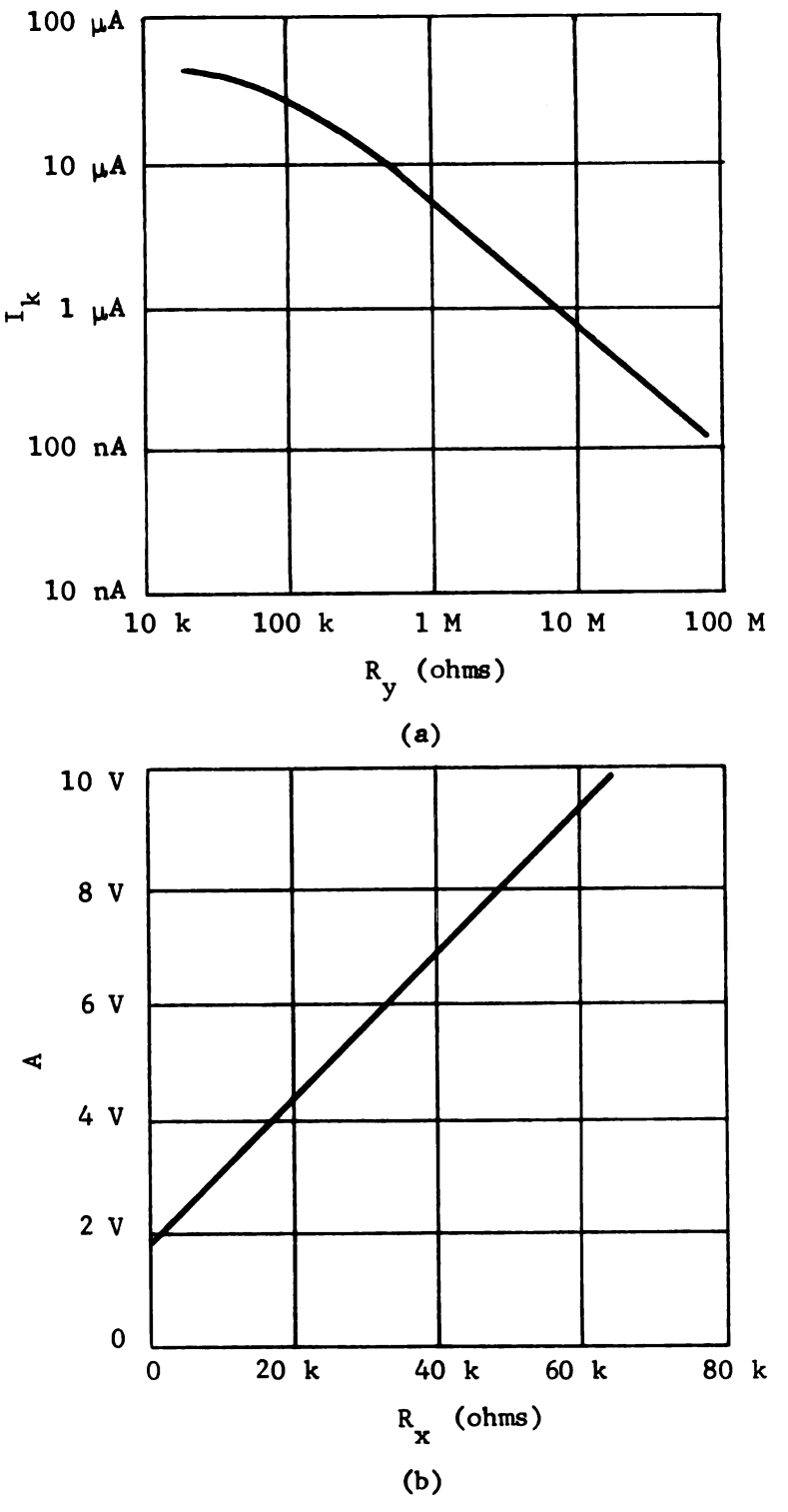


Figure A.2 Design curves for the Burr-Brown model 4116 log amplifier, (a) Reference current vs. $R_{\rm x}$, (b) Voltage constant vs. $R_{\rm x}$

$$V_{1 \text{ max}} = 10 \text{ Volts}$$
 (A.8)
 $V_{1 \text{ min}} = -A \log_{10} \frac{I_{\text{max}}}{I_{\text{k}}} = -4.5 \log_{10} \frac{60 \times 10^{-9}}{.56 \times 10^{-6}}$

$$= 4.36 \text{ Volts}$$
 (A.9)

The design parameters of the logarithmic amplifier may be summarized where

A = 4.5 Volts

$$R_y = 28$$
. k Ohms
 $I_k = .56 \mu A$
 $R_x = 11.3 \text{ M Ohms}$
Input Range $(i_s(t))$ 3nA to 60nA
Output Range $(v_1(t))$ 10V to 4.36V

APPENDIX B

DETERMINATION OF THE RAMP FREQUENCY COMPONENTS

APPENDIX B

DETERMINATION OF THE RAMP FREQUENCY COMPONENTS

The ideal output of the logarithmic amplifier in the circuit of Figure 3.4 is a linear ramp function of the form

$$v_1(t) = -A \log_{10} \frac{I_0}{I_k} - \frac{At}{\theta_p} \log_{10} e$$
 (3.14)

Differentiation of this function will yield a d-c voltage where

$$V_{2} = -R_{2}C_{1} \frac{d}{dt} v_{1}(t) = -R_{2}C_{1} \frac{d}{dt} (-A \log_{10} \frac{I_{0}}{I_{k}} - \frac{At}{\theta_{p}} \log_{10} e)$$

$$= \frac{R_{2}C_{1}A}{\theta_{p}} \log_{10} e$$
(3.15)

In order to obtain the true differential as in Equation (3.15) it is necessary to differentiate all frequencies of the ramp function $\mathbf{v}_1(t)$. This therefore requires the knowledge of the range of ramp frequency components.

The highest frequency components occur when the ramp function is on for the shortest period of time. This corresponds to a reactor stable period of ten seconds.

The "on" time for this ramp may be found by substituting the limits of $i_s(t)$ into Equation (1.1) and solving for θ_t where

$$I_{\text{max}} = I_{\text{min}} e^{\theta_t/\theta_{\text{p min}}}$$
 (1.1)

or

$$60 \times 10^{-9} = 3 \times 10^{-9} e^{\theta_t/10}$$

 $\theta_r = 10 \ln 20 \approx 30 \text{ seconds}$

The Fourier series half-range cosine expansion for f(x) = x as a recurrent triangular wave is

$$f(x) = x = \frac{k}{2} - \frac{4k}{\pi} \left(\cos\frac{\pi x}{k} + \frac{1}{9}\cos\frac{3\pi x}{k} + \frac{1}{25}\cos\frac{5\pi x}{k} + \dots + \frac{1}{(2n-1)^2}\cos\frac{(2n-1)\pi x}{k}\right) \quad 0 < x < k$$

$$n = 1, 2, \dots$$
(B.1)

Substituting the ramp function of Equation (3.14) for $f(x) \quad \text{the Fourier series expansion for} \quad v_1(t) \quad \text{is}$

$$v_{1}(t) = -A \log_{10} \frac{I_{0}}{I_{k}} \frac{At}{\theta_{p}} \log_{10} e = -A \log_{10} \frac{I_{0}}{I_{k}} - \frac{\theta_{t}}{2} \frac{A \log_{10} e}{\theta_{p \min}} - \frac{4\theta_{t}A}{2\theta_{p \min}} - \frac{4\theta_{t}A}{\theta_{t}} \log_{10} e \left(\cos \frac{\pi t}{\theta_{t}} + \frac{1}{9} \cos \frac{3\pi t}{\theta_{t}} + \frac{1}{25} \cos \frac{5\pi t}{\theta_{t}} + \frac{1}{49} \cos \frac{7\pi t}{\theta_{t}} + \frac{1}{81} \cos \frac{9\pi t}{\theta_{t}} + \frac{1}{121} \cos \frac{11\pi t}{\theta_{t}} + \dots + \frac{1}{(2n-1)^{2}} \cos \frac{(2n-1)\pi t}{\theta_{t}}\right) \qquad 0 < t < \theta_{t} = 30 \text{ sec.}$$

$$n = 1, 2, \dots \qquad (B.2)$$

The radian frequency components for the minimum duration ramp and the respective amplitudes of each (P_i) can be determined from Equation (B.2). The values are

Samuel M. Selby, <u>CRC Standard Mathematical Tables</u> (Cleveland, Ohio: The Chemical Rubber Co., 1960), p. 147.

$$\begin{aligned} \omega_1 &= \frac{\pi}{\theta_t} = 0.1048 \text{ rad/sec}, \quad P_1 &= \frac{4\theta_t A \log_{10} e}{\pi^2 \theta_{p \text{ min}}} = 7.9 \\ \omega_3 &= \frac{3\pi}{\theta_t} = 0.314 \text{ rad/sec}, \quad P_3 &= \frac{4\theta_t A \log_{10} e}{9\pi^2 \theta_{p \text{ min}}} = 0.878 \\ \omega_5 &= \frac{5\pi}{\theta_t} = 0.524 \text{ rad/sec}, \quad P_5 &= \frac{4\theta_t A \log_{10} e}{25\pi^2 \theta_{p \text{ min}}} = 0.316 \\ \omega_7 &= \frac{7\pi}{\theta_t} = 0.734 \text{ rad/sec}, \quad P_7 &= \frac{4\theta_t A \log_{10} e}{49\pi^2 \theta_{p \text{ min}}} = 0.161 \\ \omega_9 &= \frac{9\pi}{\theta_t} = 0.943 \text{ rad/sec}, \quad P_9 &= \frac{4\theta_t A \log_{10} e}{81\pi^2 \theta_{p \text{ min}}} = 0.0975 \end{aligned}$$

 $\omega_{11} = \frac{11\pi}{\theta_t} = 1.15 \text{ rad/sec}, \quad P_{11} = \frac{4\theta_t A \log_{10} e}{121\pi^2 \theta_{n,min}} = 0.0653$

Since the amplitudes of higher frequency components are less than 1/144 of the amplitude of ω_1 it is reasonable to omit them from the analysis. The value of ω_{11} is therefore the highest radian frequency to be differentiated.

APPENDIX C

DESIGN OF THE DIFFERENTIATOR

APPENDIX C

DESIGN OF THE DIFFERENTIATOR

Figure C.1 is a magnitude plot for the real and imaginary components of an ideal differentiator whose transfer function is

$$\frac{V_{\text{out}}(\omega)}{V_{\text{in}}(\omega)} = jK\omega \tag{C.1}$$

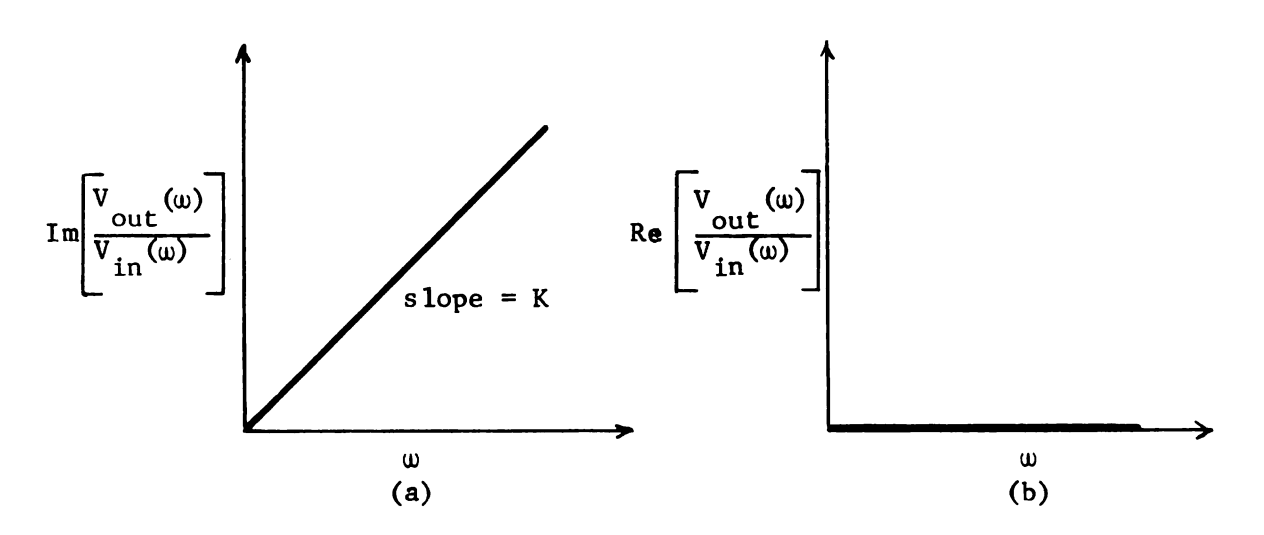


Figure C.1 Transfer function plot for an ideal differentiator,
(a) Imaginary part, (b) Real part

A differentiator circuit with the type of transfer function in Equation (C.1) has the disadvantage of enhancing noise.

If the range of frequencies to be differentiated is limited, it is possible to reduce unwanted noise by using a compensated differentiator whose transfer function is

Albert S. Jackson, Analog Computation (New York: McGraw-Hill Book Co., 1960), p. 147.

$$\frac{V_{\text{out}}(\omega)}{V_{\text{in}}(\omega)} = \frac{jK\omega}{(jK\omega + 1)(jK\omega + 1)}$$
 (C.2)

where

$$Re \left[\frac{V_{\text{out}}(\omega)}{V_{\text{in}}(\omega)} \right] = \frac{2K_{\omega}^{2}^{2}}{(1 - K_{\omega}^{2})^{2} + 4K_{\omega}^{2}^{2}}$$
 (C.3)

and

$$Im \left[\frac{V_{\text{out}}^{(\omega)}}{V_{\text{in}}^{(\omega)}} \right] = \frac{jK_{\omega}(1 - K_{\omega}^{2})}{(1 - K_{\omega}^{2})^{2} + 4K_{\omega}^{2}}$$
 (C.4)

These real and imaginary components are plotted in Figure C.2.

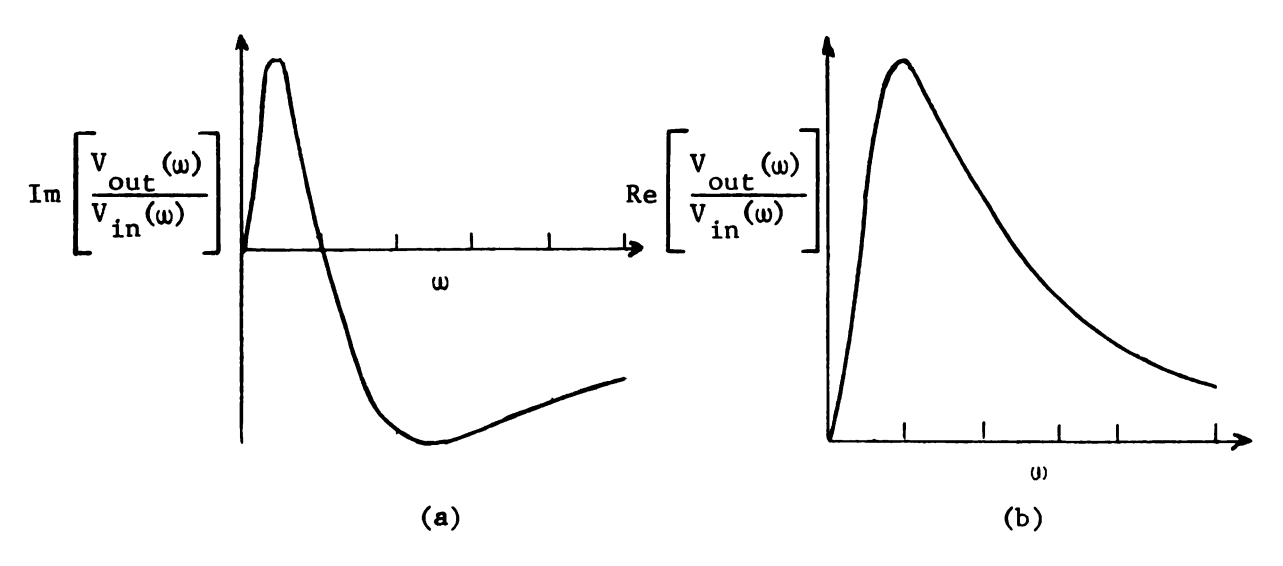


Figure C.2 Transfer function plot for a compensated differentiator, (a) Imaginary part, (b) Real part

In Appendix B it was determined that the maximum radian frequency to be differentiated in the linear ramp function was $\omega_{11} = 1.15 \text{ rad/sec.}$ It is therefore desirable to make 1/K greater than 1.15 rad/sec.

Figure C.3 is a circuit diagram of the differentiator. 20

RCA Linear Integrated Circuits (RCA, 1967), pp. 75-78.

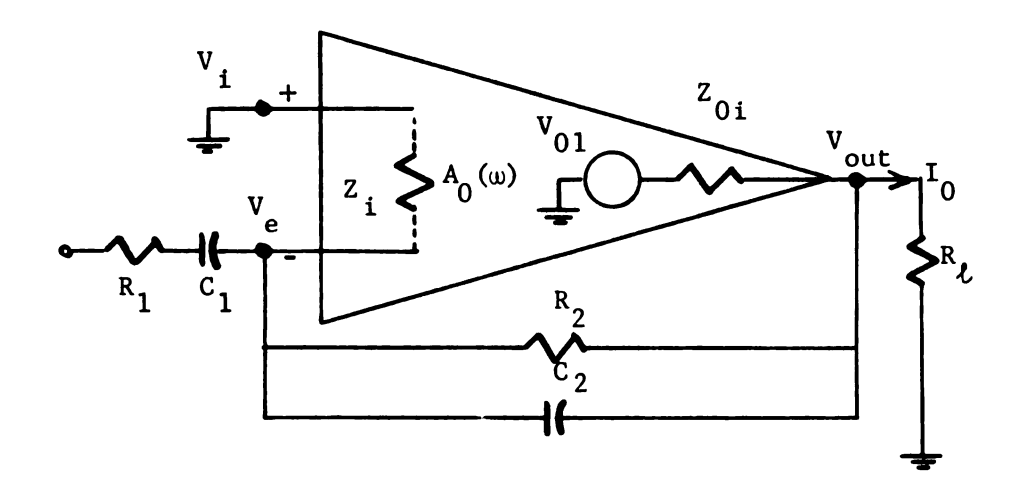


Figure C.3 Equivalent circuit of a compensated differentiator

The transfer function may be derived as follows:

Define:

$$z_f = R_2//C_2 = \frac{R_2}{j\omega R_2 C_2 + 1}$$
 (C.5)

$$Z_r = R_1 + \frac{1}{j\omega C_1}$$
 (C.6)

 v_e , v_i and v_{01} may be written as

$$V_{e} = V_{in} \frac{(Z_{f} + Z_{0i})//Z_{i}}{Z_{r} + (Z_{f} + Z_{0i})//Z_{i}} + \frac{V_{01}(Z_{r}//Z_{i})}{Z_{f} + Z_{0i} + Z_{r}//Z_{i}}$$
(C.7)

$$v_i = 0 \tag{C.8}$$

$$V_{01} = -A_0(\omega) (V_e - V_i)$$
 (C.9)

Substitution of $\,{\rm V}_{e}^{}\,$ and $\,{\rm V}_{i}^{}\,$ into the expression for $\,{\rm V}_{01}^{}\,$ yields

$$V_{01} = \frac{-V_{in}^{A_0(\omega)}(Z_f + Z_{0i})Z_i}{(Z_f + Z_{0i})Z_i + Z_r(Z_f + Z_{0i} + Z_i) + A_0(\omega)Z_iZ_r}$$
(C.10)

If $R_{\ell} \to \infty$ the exact expression for the transfer function can be written as

$$\frac{V_{\text{out}}}{V_{\text{in}}} = \frac{Z_{0i}Z_{i} - A_{0}(\omega)Z_{i}Z_{f}}{A_{0}(\omega)Z_{i}Z_{r} + (Z_{f} + Z_{0i})Z_{i} + Z_{r}(Z_{f} + Z_{0i} + Z_{i})}$$
(C.11)

This expression may be simplified if the following assumptions are made:

Assume:

$$Z_{i} \gg Z_{f}//Z_{r} \tag{C.12}$$

$$z_{0i} \ll z_{f} \tag{C.13}$$

$$Z_f \ll A_0(\omega)$$
 (C.14)

$$Z_r \ll A_0(\omega)$$
 (C.15)

Equation (C.9) may then be written 21

$$\frac{V_{\text{out}}}{V_{\text{in}}} = \frac{-Z_{\text{f}}}{Z_{\text{r}}} \tag{C.16}$$

When the expressions for $\mathbf{Z}_{\mathbf{r}}$ and $\mathbf{Z}_{\mathbf{f}}$ are substituted into this equation the differentiator transfer function becomes

$$\frac{v_{\text{out}}}{v_{\text{in}}} = \frac{-jR_2C_1\omega}{(jR_1C_1\omega + 1)(jR_2C_2\omega + 1)}$$
(C.17)

If $R_1C_1 = R_2C_2$ then the magnitude plot in Figure C.2 will correspond to Equation (C.17) with $1/K = 1/R_1C_1$.

For a differentiator error of one percent maximum it is necessary to establish a corner frequency about ten times the maximum frequency to be differentiated. In other words

$$\frac{1}{R_1C_1} = \frac{1}{R_2C_2} = 10 \omega_{\text{max}} = 10 \omega_{11}$$
 (C.18)

^{21 &}lt;u>Ibid.</u>, pp. 75-78.

where $\omega_{11} = 1.15 \text{ rad/sec}$ and was determined in Appendix B.²²

A trade off of accuracy vs. noise is encountered if Equation (C.18) is used to design the differentiator. The prupose of the low-pass filter in Figure 3.4 is to attenuate the noise passed by the differentiator. It was discovered that for $1/R_1C_1 = 10 \omega_{11} = 11.5 \text{ rad/sec}$ the filter could not effectively reduce the noise without causing an excessive delay in the d-c response due to its long time constant. A decision was made to limit the filter time constant to 0.6 second. This meant the corner frequency of the differentiator had to be reduced until the noise level was tolerable. The experimental resultant corner frequency was $1/R_1C_1 = 3.8 \text{ rad/sec}$ or about three times as great as the highest frequency to be differentiated.

The magnitude of the error caused by inexact differentiation of the maximum ramp frequency will be small since the amplitude of this frequency component is only 1/121 of the major ramp frequency.

Jackson, Analog Computation, p. 147.

APPENDIX D
DESIGN OF THE FILTER

APPENDIX D

DESIGN OF THE FILTER

Figure D.1 is a schematic of the output filter in Figure 3.4.

The filter is a simple RC low-pass filter with a unity gain output buffer stage to prevent loading.

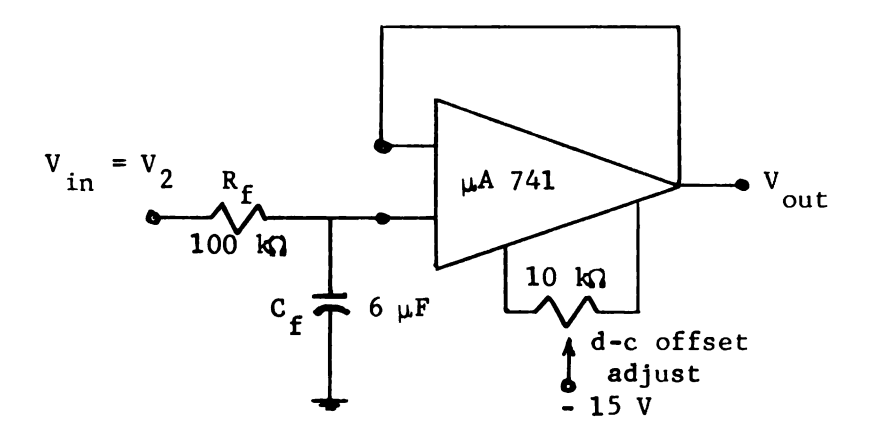


Figure D.1 Output filter for the reactivity meter

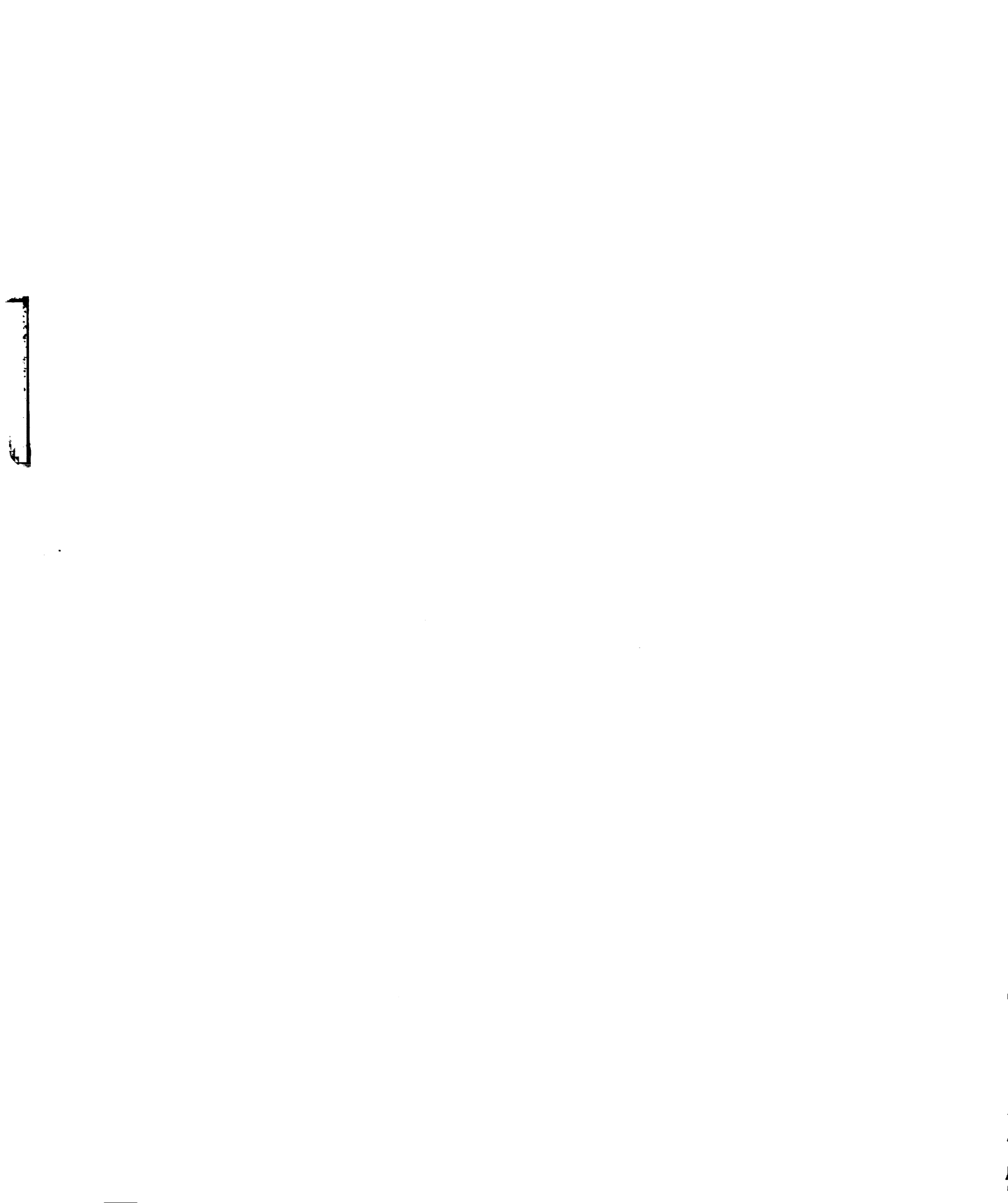
The transfer function for the filter is

$$\frac{V_{\text{out}}(\omega)}{V_{\text{in}}(\omega)} = \frac{1}{jR_fC_f\omega + 1}$$
 (D.1)

Since the output voltage of the differentiator (V_2) is a d-c voltage with superimposed low-frequency noise it is desirable to make the filter time constant long enough to reduce this noise

while at the same time have a reasonable response time to the d-c voltage.

Final tests of the reactivity meter indicated that a filter time constant of $R_f^c = 0.6$ seconds reduced the output noise level on the meter to less than ± 0.4 percent full scale. This value for R_f^c also gave a d-c response time of about 3 seconds.



APPENDIX E

SPECIFICATIONS OF THE COMPENSATED ION CHAMBER

APPENDIX E

SPECIFICATIONS OF THE COMPENSATED ION CHAMBER

The TRIGA Mark I nuclear reactor at Michigan State University contains a Westinghouse type WL-8501 compensated ion chamber. Table E.1 tabulates the specifications of this chamber.

Table E.1 Specifications of the Westinghouse type WL-8501 Compensated ion chamber

Maximum Voltage Between Electrodes (dc)1000 V
Operating Voltage for Boron Chamber (dc) 580 V
Operating Voltage for Gamma Chamber (dc) 0 to -37 V
Output Resistance, Signal to Case, Minimum10 13 Ohms
Output Capacitance, Signal to Case, Approximately130 pF
Thermal Neutron Flux Range2.5×10 ² to 1.5×10 ¹⁰ n/cm ² /sec
Thermal Neutron Sensitivity
Gamma Sensitivity, Compensated2.5×10 ⁻¹³ A/R/hr

Since the output resistance of the ion chamber is greater than $10^{13}\,$ Ohms the chamber may be treated as a current source.

Westinghouse WL-8501 (New York: Westinghouse Electric Co., 1965), pp. 1-2.

MICHIGAN STATE UNIV. LIBRARIES
31293105898724